



# Michigan Ion Beam Laboratory

FOR SURFACE MODIFICATION AND ANALYSIS

---

## ANNUAL RESEARCH REPORT

# 2013

Gary S. Was, Director  
Ovidiu Toader, Operations Manager  
Fabian Naab, Engineer

2600 Draper Road  
Department of Nuclear Engineering and Radiological Sciences  
University of Michigan  
Ann Arbor, Michigan 48109-2145  
<http://www.ners.engin.umich.edu/research/mibl/>

Telephone: (734) 936-0166

Fax: (734) 763-4540

## ***The Annual Research Report***

This report summarizes the principal research activities in the Michigan Ion Beam Laboratory during the past calendar year. Eighty-three researchers conducted thirty-four projects at MIBL that accounted for over 4800 hours of equipment usage. The programs included participation from researchers at the University, corporate research laboratories, private companies, government laboratories, and other universities across the United States. The extent of participation of the laboratory in these programs ranged from routine surface analysis to ion assisted film formation. Experiments included Rutherford backscattering spectrometry, elastic recoil spectroscopy, nuclear reaction analysis, direct ion implantation, ion beam mixing, ion beam assisted deposition, and radiation damage by proton bombardment. The following pages contain a synopsis of the research conducted in the Michigan Ion Beam Laboratory during the 2012 calendar year.

### ***About the Laboratory***

The Michigan Ion Beam Laboratory for Surface Modification and Analysis was completed in October of 1986. The laboratory was established for the purpose of advancing our understanding of ion-solid interactions by providing up-to-date equipment with unique and extensive facilities to support research at the cutting edge of science. Researchers from the University of Michigan as well as industry and other universities are encouraged to participate in this effort.

The lab houses a 1.7 MV tandem ion accelerator, a 400 kV ion implanter, and an ion beam assisted deposition (IBAD) system. Additional facilities include a vacuum annealing furnace, a surface profilometry system, and a scanning laser surface curvature measurement system. The control of the parameters and the operation of these systems are mostly done by computers and are interconnected through a local area network, allowing off-site monitoring and control.

In 2010, MIBL became a Partner Facility of the Advanced Test Reactor, National Scientific User Facility (ATR-NSUF), at Idaho National Laboratory, providing additional opportunities for researchers across the US to access the capabilities of the laboratory. In its first two years as a Partner Facility, MIBL hosted nine ATR projects.

Respectfully submitted,

A handwritten signature in black ink, appearing to read "Gary S. Was". The signature is written in a cursive style with a large initial "G".

Gary S. Was, Director

# **RESEARCH PROJECTS**

# IRRADIATION EFFECTS IN FERRITIC-MARTENSITIC STEELS AT VERY HIGH DOSES

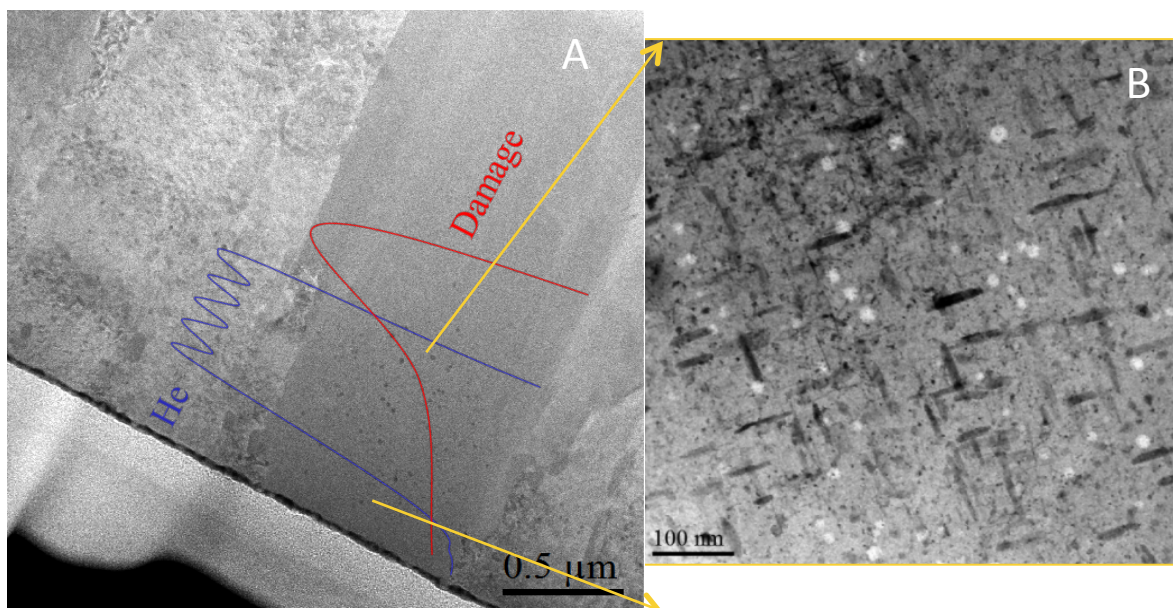
E.M. Beckett, J.P. Wharry, Z. Jiao, K. Sun, G.S. Was

Department of Nuclear Engineering and Radiological Sciences, University of Michigan

This project focuses on the effects of very high doses of self-ion irradiation, up to 500 dpa, in HT9 and other ferritic-martensitic (F-M) steels, in the range of 400-500°C, which is the anticipated operating temperature regime of the TerraPower, LLC traveling wave reactor. Of greatest interest is the microstructural evolution under irradiation, including void swelling, dislocation loop nucleation and growth, and precipitation.

Self-ion irradiation experiments have been performed on ferritic-martensitic alloy HT9 to determine swelling behavior at 440°C to doses of 280 dpa and above using two different helium pre-implantation conditions. Irradiations were performed on both helium implanted and unimplanted samples using raster scanning on a Tandatron accelerator at the Michigan Ion Beam Lab. The effects of helium pre-implantation on bulk swelling were determined by examining the void distribution using transmission electron microscopy (TEM) and in samples implanted with 0, 10 and 100 atom parts per million (appm) helium. Additionally, atom probe tomography (APT) was used to examine the effect of helium on precipitate formation. Helium implantation was not required to form voids at doses of 280 dpa and above. The addition of helium increased average size, void density and void swelling. Void density was most affected by the addition of helium as helium greatly enhances void nucleation, but the effect of growth is less clear. There was no significant effect of helium implantation on precipitate nucleation. Swelling reached a maximum of 0.81% in samples implanted with 100 appm He and irradiated to 375 dpa at 440°C.

This work is supported by TerraPower, LLC.



Self-ion damage profile and helium implant zone (dark field image) (left) and voids within helium pre-implanted zone (bright field image) (right).

# ACCELERATOR BASED STUDY OF IRRADIATION CREEP IN GRAPHITE

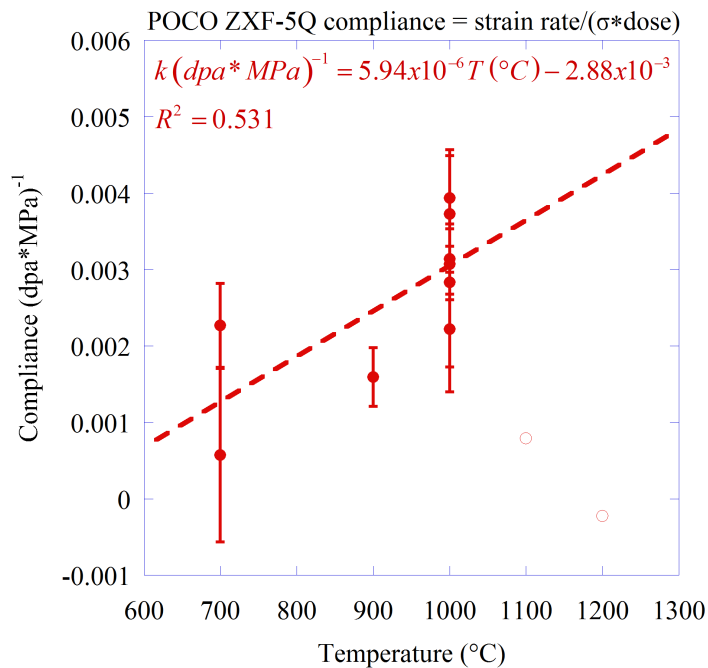
A.A. Campbell and G.S. Was,

Department of Nuclear Engineering and Radiological Sciences, University of Michigan

This work has focused on performing proton irradiation induced creep experiments on ultra-fine grain graphite. Graphite is the primary structural component in the Gen-IV Very High Temperature Reactor (VHTR).

Irradiation creep experiments were systematically performed to study the effect of applied tensile stress, irradiation dose rate, and irradiation temperature, on the creep behavior of this graphite. For the stress dependence experiments, which were performed with 3MeV protons at 1000°C and dose rate of  $\sim 1.15 \times 10^{-7}$  dpa/s, the creep rate varied linearly with stress. For the dose rate dependence experiments, which were performed with 3MeV protons at 700°C and tensile stress of 20MPa, the creep rate was linear with dose rate. For the temperature dependence experiments, which were performed with 3MeV protons tensile stress of 20MPa and with a varied dose rate to achieve the desired temperature, the creep compliance varied linearly with temperature. The creep compliance is used for temperature dependence to account for the different dose rate and applied stress. The figure below shows the summary of the temperature dependence experiments and highlights the linear dependence of creep compliance on temperature.

This work is supported by the U.S. Department of Energy under NERI grant DE-FC07-06ID14732, and INL under contract DE-AC07-05ID14517.



Temperature dependence of creep compliance. Compliance was calculated by dividing strain rate measured by the Laser Speckle Extensometer by applied tensile stress and dose rate.

# OXYGEN INCORPORATION IN ZnTe:O/GaAs GROWN BY PLASMA ASSISTED MOLECULAR BEAM EPITAXY

C. Chen<sup>1</sup>, F. Naab<sup>2</sup>, J. D. Phillips<sup>1</sup>

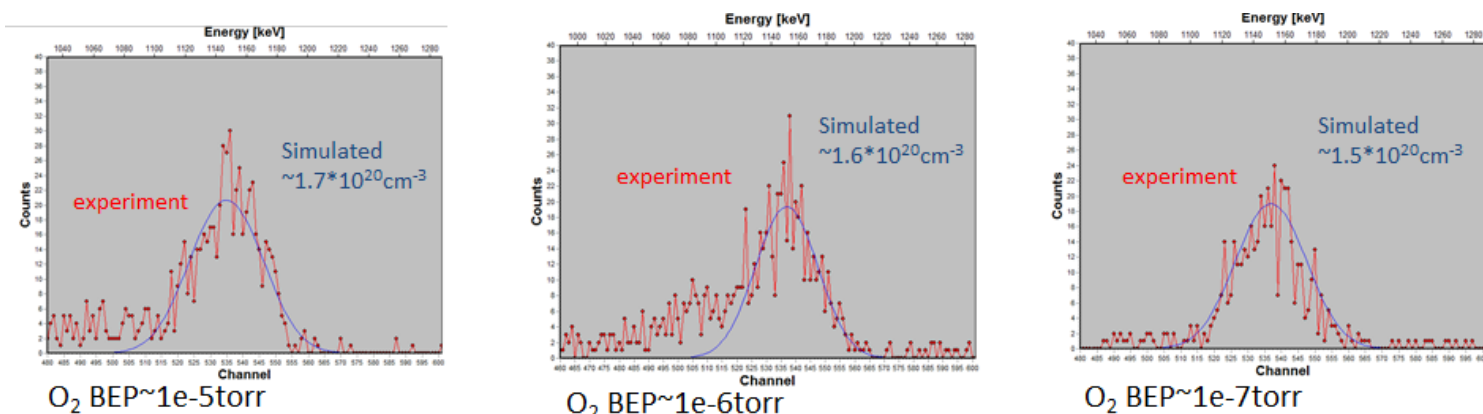
<sup>1</sup>Department of Electrical Engineering and Computer Science, University of Michigan

<sup>2</sup>Department of Nuclear Engineering and Radiological Sciences, University of Michigan

Incorporation of oxygen into substitutional sites in ZnTe leads to a deep electronic state about 0.4eV below the conduction bandgap of ZnTe. One proposed application of this material is for use as a sub-bandgap absorber in intermediate band solar cells, which have been shown theoretically to have a thermodynamic limiting efficiency of 63%.

As part of an effort to increase oxygen content to enhance light absorption, oxygen concentrations of samples prepared by different growth conditions were derived from nuclear reaction analysis of the  $O^{16}(d,p)O^{17}$  reaction in this work. The fits were analyzed with the software SIMNRA, and the results showed the oxygen concentration to be around  $10^{20} \text{ cm}^{-3}$  for materials prepared with different oxygen background pressures of  $10^{-7}$ ,  $10^{-6}$ , and  $10^{-5}$  Torr during growth. The apparent independence between total oxygen incorporation and growth conditions has been separately confirmed by SIMS measurements. Future work could include channeling studies to investigate the relationship between growth conditions and oxygen dopant location within the ZnTe semiconductor matrix.

This work is supported as part of the Center for Solar and Thermal Energy Conversion, an Energy Frontier Research Center funded by the U.S. Department of Energy, Office of Science, Office of Basic Energy Sciences under Award Number DE-SC0000957.



Nuclear reaction analysis data of the  $O^{16}(d,p)O^{17}$  reaction for ZnTe:O/GaAs prepared with the oxygen plasma background pressures of  $10^{-7}$  Torr (left),  $10^{-6}$  Torr (middle),  $10^{-5}$  Torr (right). Analysis with SIMNRA software results in the oxygen concentration estimate of  $10^{20} \text{ cm}^{-3}$  for these three growth conditions

# MEASUREMENT OF Bi CONTENT IN GaSb<sub>x</sub>Bi<sub>1-x</sub> FILMS GROWN BY MOLECULAR BEAM EPITAXY

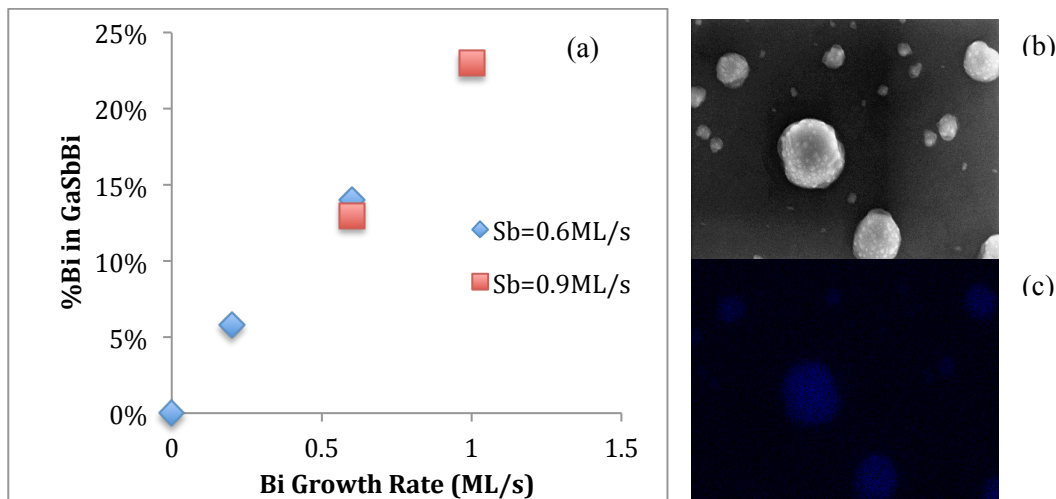
A. Duzik, J. M. Millunchick

Department of Materials Science and Engineering, University of Michigan

Bi-containing III-V alloys has gained more interest in the last decade given its strong ability for band gap reduction, but research has focused on GaAsBi grown with molecular beam epitaxy (MBE). GaSbBi offers an alternative to the difficulties of incorporating Bi into GaAs; the large lattice constant of GaSb permits large Bi atoms to more easily occupy GaSb lattice sites. Several of the MBE-grown, 300nm GaSbBi films were grown with various growth rates of Ga, Sb, and Bi at a GaSb substrate temperature of 300°C. RBS measurements were done with 2MeV He<sup>++</sup> ions to determine the Bi content, if any, in these films.

For a fixed Ga rate of 0.6ML/s and Sb rates of 0.6ML/s and 0.9ML/s, the amount of Bi detected in the GaSbBi film is plotted below (Fig. 1a) as a function of Bi growth rate. The Bi content was determined by fitting to the RBS spectra using the SimNRA software. Only a handful of samples have been grown and analyzed, but preliminary results show a clear increase in Bi content with increasing Bi growth rate. However, the contents are likely overestimated, as SEM analysis of the film surfaces show large, Bi-rich droplets on the films (Fig. 1b-c). Efforts to eliminate these droplets during growth are ongoing, in order to obtain a more accurate composition.

This work was performed, in part, at the Center for Integrated Nanotechnologies, a U.S. Department of Energy, Office of Basic Energy Sciences user facility at Los Alamos National Laboratory (Contract DE-AC52-06NA25396) and Sandia National Laboratories (Contract DE-AC04-94AL85000). The authors gratefully acknowledge the support of the National Science Foundation Materials World Network DMR 0908745. AJD acknowledges funding from the National Science Foundation IGERT program DGE 0903629. Any opinions, findings, and conclusions or recommendations expressed in this material are those of the author(s) and do not necessarily reflect the views of the National Science Foundation.



Plot of Bi content in GaSbBi films (a), secondary SEM (b), and Bi backscatter image of GaSbBi surface droplets (c).

# SILICON CARBIDE COATING VIA POLYMERIC PYROLYSIS

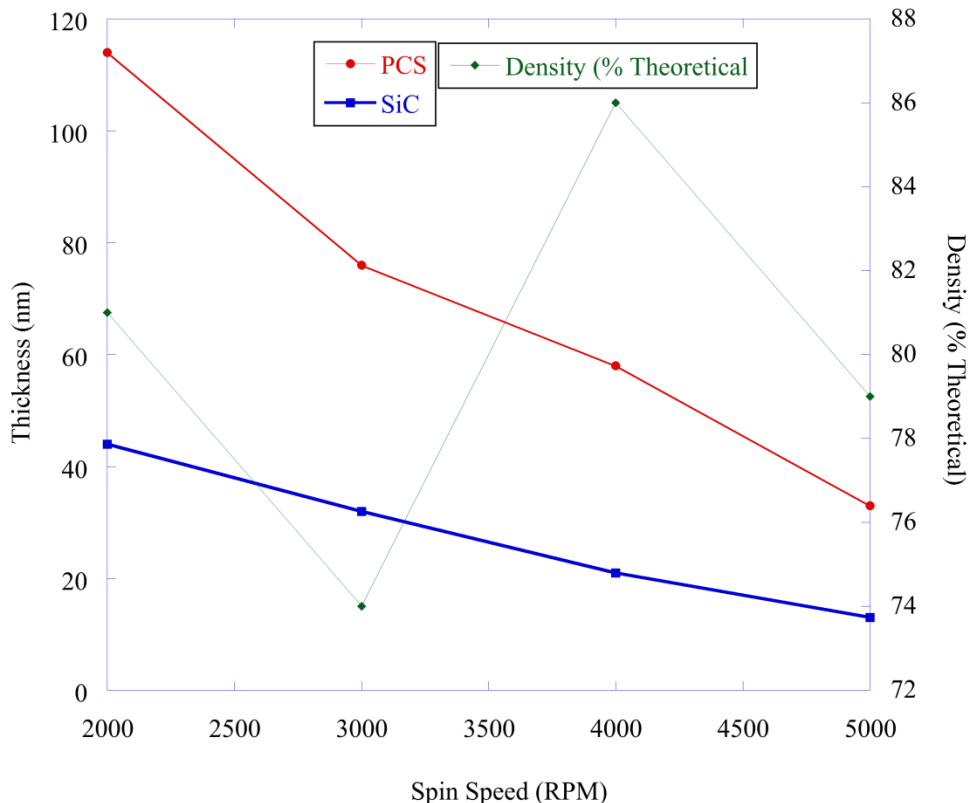
S. Dwaraknath, G.S. Was

Department of Nuclear Engineering and Radiological Sciences, University of Michigan

This work focused on calibrating a coating process for the deposition of thin films of SiC. A class of polymers called polycarbosilane (PCS) is diluted in a solvent such as toluene and then spun onto the substrate. Several parameters affect this process along with spin speed and spin time. Creating very thin coatings poses the problem of measuring thickness. Ellipsometry can be used to measure the polymer coating, but the optical constants of the amorphous SiC are unknown, resulting in the need for a sanity check.

Rutherford backscattering spectroscopy (RBS) is capable of measuring layer thickness with a high degree of accuracy, but it is incapable of discerning crystallography. SiC substrates were first coated with PyC before being coated via the spin coating process with PCS obtained from STARFIRE Ceramics inc. Parameters were varied until suitable coatings were obtained and then the parameter space was explored. The figure shows the calibration for spin coating 1% PCS by volume diluted in toluene, as a function of spin speed. Ellipsometry was used to measure the PCS thickness, while RBS was used to measure the pyrolyzed SiC coating.

This work is supported by the Department of Energy under NEUP Contract #00103195



Calibration of SiC thickness and density as a function of spin speed for 1% PCS diluted by volume in toluene.

# ENHANCED PHOTOVOLTAIC EFFICIENCY THROUGH HETEROJUNCTION ASSISTED IMPACT IONIZATION: SYNTHESIS OF SiC HARVESTER PARTICLES

A. Rockett, D. Hebert, J. Wang, G. Campbell

Department of Materials Science & Engineering, University of Illinois at Urbana-Champaign

Photovoltaic conversion of solar energy directly to electricity represents one of the most promising methods for supplying global energy needs in the coming years. However, the current technologies are limited in their ability to capture this energy with high efficiency. One opportunity to improve this efficiency is to produce more than one electron-hole pair via absorption of a single photon by a semiconducting medium: the quantum efficiency (QE) is greater than one. A common example is offered by avalanche photodiodes, where an externally applied bias accelerates the primary photoexcited carriers. These gain enough energy to decay by impact ionization (II) to produce secondary electron-hole pairs. Gain does not require an external bias when the photon has high enough energy, as is the case in x-ray and particle detectors. In the optical regime, however, achieving  $QE > 1$  without external bias is rare. To learn how to do this with high efficiency is an interesting fundamental challenge that will also have a profound effect on photovoltaic (PV) technologies, since it will allow the solar spectrum to be converted to electrical energy with an efficiency higher than that dictated by the Shockley-Queisser limit for a single gap absorber.

This project combines thin film synthesis, analysis, and modeling expertise to develop heterojunction-assisted impact ionization (HAI) to accomplish  $QE > 1$  in unbiased semiconducting heterostructures and nanostructured thin films. HAI combines a narrow, indirect band gap host material with wide, direct or indirect gap absorbers (harvesters) in the form of thin films, nanorods, or nanoparticles. Higher energy photons generate carriers in the wide-gap material. As these pass into the narrow-gap material, they can decay through II to produce additional carriers. We will (a) explore promising combinations of semiconducting materials with appropriate band alignments and morphology to promote HAI, (b) synthesize thin films that maximize the probability of HAI while minimizing recombination pathways, (c) characterize, model, and control band offsets between narrow and wide band gap semiconductors, (d) confirm that the materials achieve an internal  $QE > 1$  using radio frequency photoconductivity and photoluminescence measurements, (e) probe the rates of hot carrier decay near buried interfaces by II and phonon excitation using ultrafast laser techniques, and (f) develop and test robust multi-scale and continuum models of the HAI process to learn how to optimize the internal QE.

Our specific task, within this broad collaborative project, at U of I is to introduce “harvester” particles in a semiconductor matrix from which a photovoltaic device is produced that can absorb high energy photons and produce a larger amount of electric current in the output of the device than would normally be possible. The Rockett Group, including post-doctoral researcher Damon Hebert and undergraduate research assistants Jie Wang and Gavin Campbell (now at Northwestern University), aims to achieve this higher current output by introducing silicon carbide (SiC) precipitates in a silicon (Si) matrix. These particles will absorb high energy light and release high energy electrons into a surrounding Si matrix under conditions that promote the generation of two free electrons rather than the one normally generated. The research is being initiated by implantation of carbon atoms into the Si matrix (at MIBL) and subsequent annealing of the implanted Si to produce a fine distribution of SiC particles in the Si matrix at a controlled location. Subsequent annealing is being carried out in the Rockett laboratories and samples are being tested to demonstrate carrier multiplication at the University of Oregon at Eugene, which is the lead institution in this collaboration. Post-annealing sample analysis is being done by secondary ion mass spectrometry (SIMS) and x-ray diffraction (XRD). Success has the potential to significantly increase device efficiency without undue additional expense. This holds the potential to significantly reduce the

cost per kilowatt hour of the final electricity, which is crucial to achieving competitive pricing in energy generation compared to existing technologies.

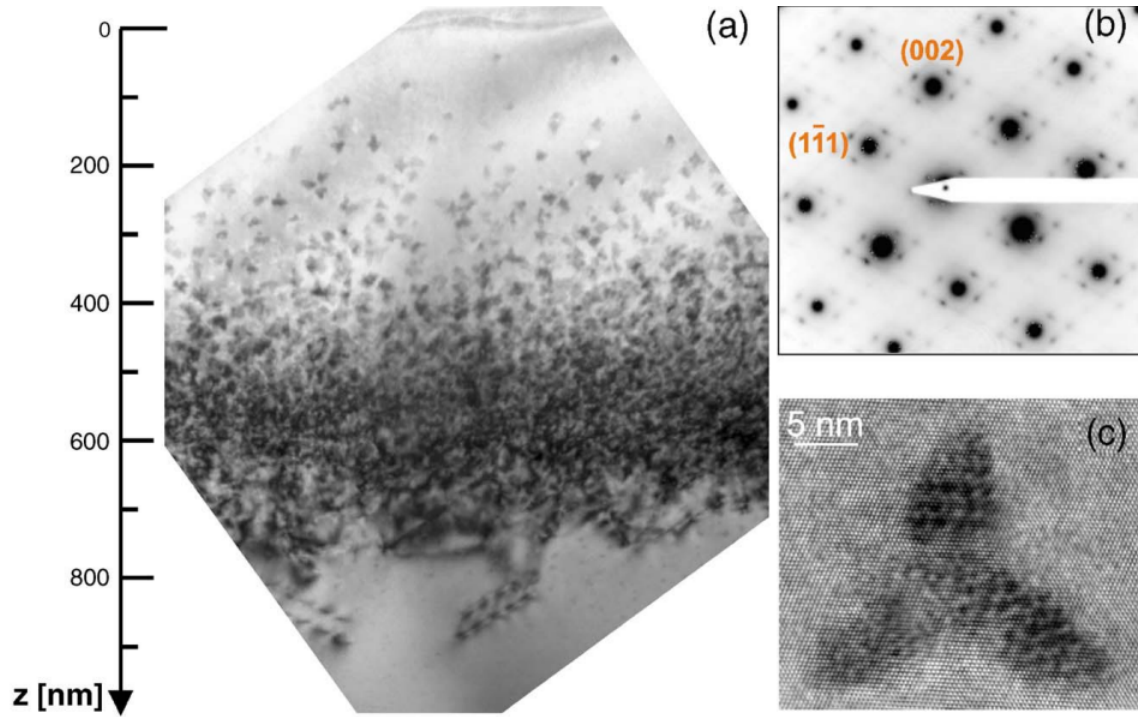


Fig. 3 (a) Cross-sectional TEM bright-field image showing precipitates and dislocations in a sample implanted at 900 C. (b) A corresponding selected area diffraction pattern of the sample in  $[110]$  orientation. The lattice resolution STEM bright-field image in (c) was taken in  $[110]$  orientation and shows one of the precipitates at a depth of about 300 nm.

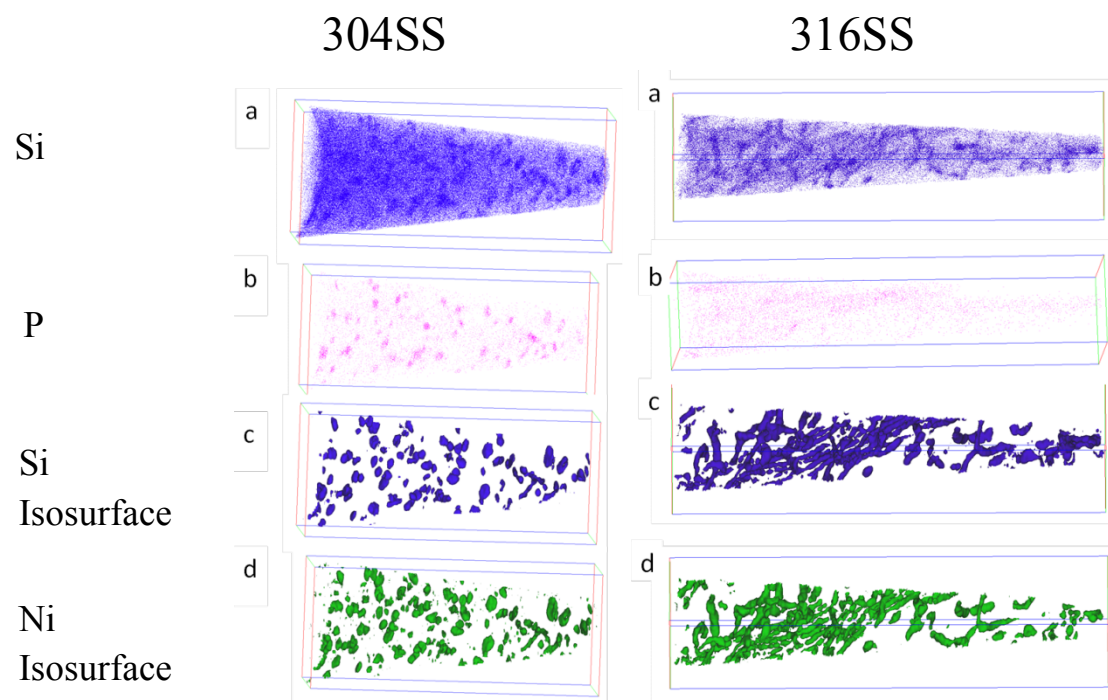
# AGING AND EMBRITTLEMENT OF HIGH FLUENCE STAINLESS STEELS

Z. Jiao and G.S. Was

Department of Nuclear Engineering and Radiological Sciences, University of Michigan

Self-ion irradiations are capable of producing samples at high fluences over a short time frame. However, microstructure and microchemistry by heavy ion irradiations need to be validated against those from neutron irradiations. The irradiated microstructure and radiation-induced segregation (RIS) of 304L and 316L SS irradiated in BOR60 to 46 dpa at 320°C was used as the reference irradiation condition. Four self-ion irradiations (46 dpa at 500°C; 30 dpa at 600°C and 46 and 260 dpa at 380°C) were chosen and conducted. Self-ion irradiation to 46 and 260 dpa at 380°C produced similar dislocation loop size and density as neutron irradiation to 46 dpa at 320°C. Self-ion irradiation to 30 dpa at 600°C produced grain boundary segregation close to the magnitude from neutron irradiation but broader. The results suggest that the best way to emulate neutron irradiated microstructure in stainless steels using self-ion irradiation may be to study microstructure evolution and RIS separately. Atom Probe Tomography reveals the difference in the morphologies of Ni/Si-rich clusters in solution annealed 304SS and cold-worked 316SS. Segregation of Si and Ni to dislocations is apparent in 316SS.

Support for this research was provided by the U.S. National Nuclear Security Administration (NNSA) under award # 91752



Formation of Ni/Si-rich precipitates in 304L SS and 316L SS following  $\text{Fe}^{++}$  irradiation to 46 dpa at 380°C as revealed by APT.

# MITIGATION STRATEGY FOR IASCC IN AUSTENITIC STAINLESS STEELS

Z. Jiao<sup>1</sup>, G.S. Was<sup>1</sup>, P. Chou<sup>2</sup>

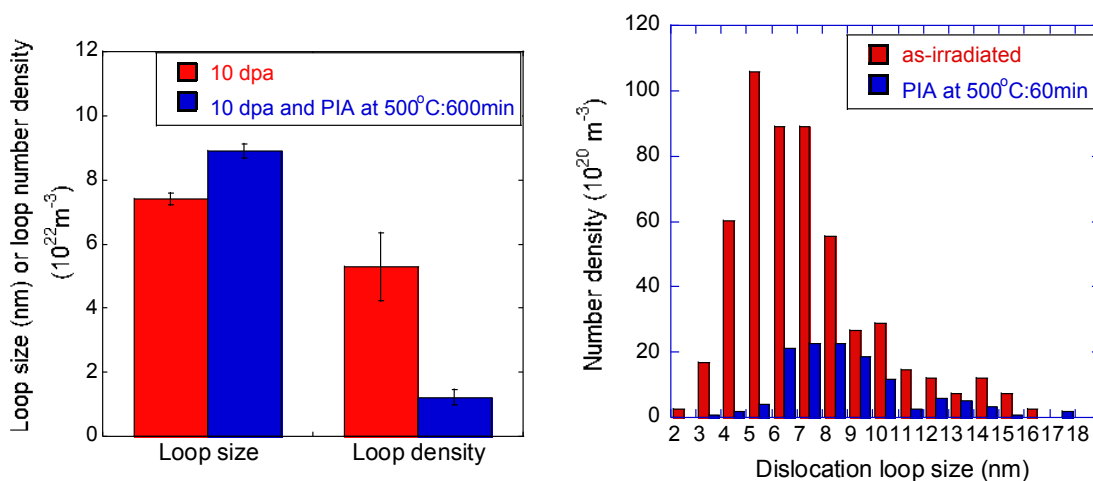
<sup>1</sup>Department of Nuclear Engineering and Radiological Sciences, University of Michigan

<sup>2</sup>Electric Power Research Institute

Irradiation assisted stress corrosion cracking (IASCC) is the primary form of core component cracking in boiling water reactors. It is also an issue of growing importance in pressurized water reactors. The ultimate goal is not only to understand the mechanism of IASCC, but to provide a mitigation strategy for components under service and a guide for alloy design for future reactors. Post-irradiation annealing (PIA) has been demonstrated as a potential mitigation method for IASCC in stainless steels in a few studies. However, the reason that PIA may lead to the mitigation of IASCC is not well understood. This project is intended to understand the mitigation mechanism of PIA through its relationship with localized deformation in proton-irradiated austenitic stainless steels.

Commercial grade 304SS that is very susceptible to IASCC in simulated BWR environment was selected for this study. Samples were irradiated to 10 dpa using 2 MeV protons at 360°C. PIA of the irradiated sample at 500°C for 60 minutes leads to a 75% reduction in the population of dislocation loops formed in the as-irradiated condition, which may contribute to the mitigation of IASCC.

Support for this research was provided by the Electric Power Research Institute (EPRI)



Comparison of dislocation loop size (diameter), density and distribution in as-irradiated (360°C:10dpa) and after PIA at 500°C for 60 minutes.

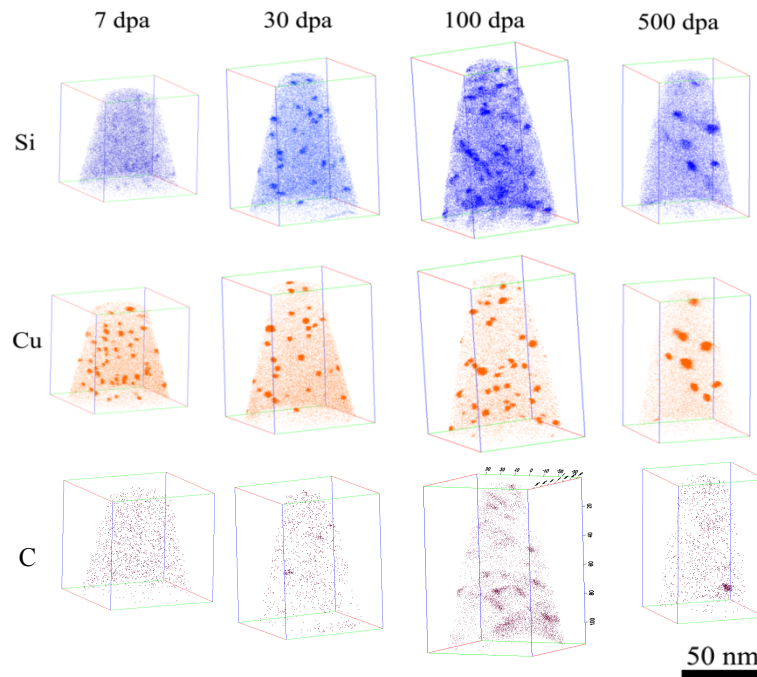
# PHASE STABILITY IN HEAVY ION IRRADIATED FERRITIC-MARTENSITIC ALLOYS AT HIGH FLUENCES

Z. Jiao, J. Wharry, E. Beckett and G.S. Was

Department of Nuclear Engineering and Radiological Sciences, University of Michigan

Understanding microstructure development in materials irradiated to high dose is, in a sense, the holy grail of materials performance in reactor systems. Fast reactor ducts will likely see damage levels of 200 dpa, and for the Traveling Wave Reactor to become a reality, the clad and some structural materials must withstand 500-600 dpa. Water-based test reactors (ATR, HFIR) can provide  $\sim 3$ -5 dpa/yr level. Fast reactors accumulate damage more quickly but are limited to  $\sim 20$  dpa/yr. As such, only ion irradiation is capable of providing the required levels of damage in reasonable time frames. Ferritic-martensitic alloys (T91, HCM12A and HT-9) were irradiated up to 500 dpa at temperatures 400-500°C at MIBL. Radiation-induced precipitates were investigated using atom probe tomography (APT). Typically, four types of precipitates were observed in heavy-ion irradiated F-M alloys. They are Ni/Si-rich, Cu-rich and Cr-rich precipitates and Cr-rich carbides. Evolution of precipitates in HCM12A following  $\text{Fe}^{++}$  irradiations at 400°C up to 500 dpa is shown in the figure.

Support for this research was provided by the U.S. DOE under contract DE-FG07-07ID14894, and DE-AC07-05ID14517.



APT Ni, Cu and C atom maps reveal the evolution of Ni/Si-rich, Cu-rich and Cr/C-rich precipitates with dose in HCM12A following  $\text{Fe}^{++}$  irradiations at 400°C up to 500 dpa.

## PROTON IRRADIATION OF AECL ALLOYX-750

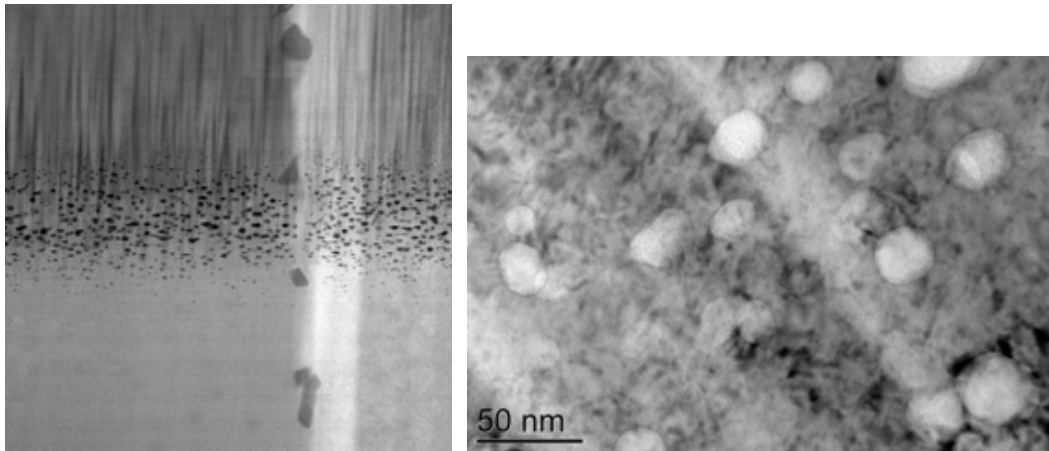
Z. Jiao<sup>1</sup>, O. Toader<sup>1</sup>, G.S. Was<sup>1</sup>, C. Judge<sup>2</sup>

<sup>1</sup>Department of Nuclear Engineering and Radiological Sciences, University of Michigan

<sup>2</sup>Atomic Energy of Canada Limited

Alloy X-750 is used as spacer material in CANDU reactor fuel channel. A key function of the spacer is to maintain the insulating gap between the pressure tube and the calandria tube. Failure of the space due to irradiation can lead to hydride blister formation and possible pressure tube rupture. To emulate irradiation damages at high doses, X-750 alloys were pre-implanted with 6000 appm He and then irradiated to 20 dpa at 250 and 380°C, respectively, using 1.2 MeV protons. Microstructure examination shows significant swelling at the peak damage (~9 $\mu$ m) but no voids at the helium implanted depth (~5 $\mu$ m) in X-750 irradiated at 380°C. Further irradiation to higher dose (40 dpa and 60 dpa) is been conducted and will completed in early 2013.

Support for this research was provided by the Atomic Energy of Canada Limited (AECL)



Void swelling in AECL X-750 at the peak damage following proton irradiation to 20 dpa (plateau) at 380°C.

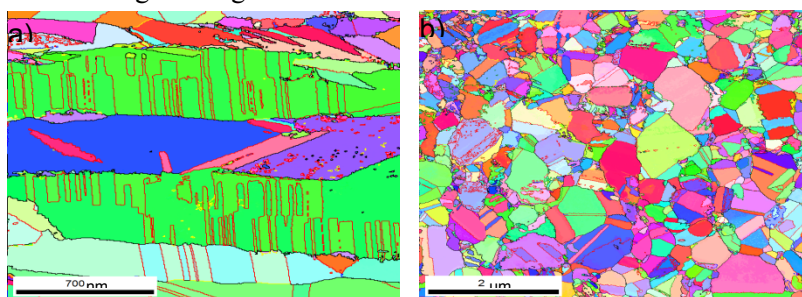
# DEVELOPING A MECHANISTIC UNDERSTANDING OF RADIATION TOLERANT MATERIALS

T. LaGrange, M. Kumar,  
Lawrence Livermore National Laboratory

The materials in future nuclear reactors, particularly those using proliferation-resistant high-burn-up fuels, will be required to perform for extended periods under extreme conditions of temperature and radiation that will lead, at best, to a slowly evolving microstructure or, at worst, a radically modified microstructure. High-energy particle radiation will continually produce defects that will be mobile at high temperatures and will move under the influence of the stress fields associated with pre-existing extended defects. After an initial relaxation phase in which many of the point defects recombine, the interstitials, being more mobile than the vacancies, are quickly absorbed by nearby dislocations. This can induce creep by dislocation climb and also cause dislocation multiplication resulting in work hardening and embrittlement. The small excess of vacancies left behind can build up, leading to void formation and swelling. Even a small imbalance can eventually lead to a dramatic degradation of strength and structural integrity.

The long-term stability of a microstructure under irradiation depends on its neutrality toward defect absorption. Nanocrystalline microstructures with a high interfacial areal density of sites that can act as sinks for the point defects could be considered as ideal radiation-resistant materials. But through either normal or radiation-accelerated grain coarsening processes, the grain boundary (GB) area per unit volume tends to decrease with time, eventually negating the radiation resistance advantages of the starting material. Indeed this has been shown for the case of nanostructured thin films of Cu, Ni, Fe and other materials, where a thermal spike associated with a cascade locally affects an area of the same dimensions as the grain size and enables grain growth. This could be particularly the case in radiation environments of high doses and dose rates, where the balance between rate of defect production and absorption may always be biased toward the former and may overwhelm even an excellent defect sink. Remarkably, little is known of the basic physics of coarsening in high-radiation environments, so with current knowledge it is difficult to predict whether a given nanostructured material will have adequate radiation resistance over its planned service lifetime. In this work we aim to study how statistically different grain boundary networks in nanocrystalline Cu (as shown below) influences radiation damage and adverse coarsening processes in high radiation environments.

The work presented in this article was performed at LLNL under the auspices of the U.S. Department of Energy by Lawrence Livermore National Laboratory under Contract DE-AC52-07NA27344 and supported fully by the U.S. Department of Energy, Office of Basic Energy Sciences, Division of Materials Sciences and Engineering.



Orientation and grain boundary maps of nanotwinned columnar copper foil (left), and nanocrystalline copper foil having equiaxed grains that are internally twinned (right). High angle boundaries with a misorientation  $>15^\circ$  are colored black, low angle boundaries  $<15^\circ$  are colored yellow, and  $\Sigma 3$  and  $\Sigma 9$  CSL boundaries are colored red and blue, respectively.

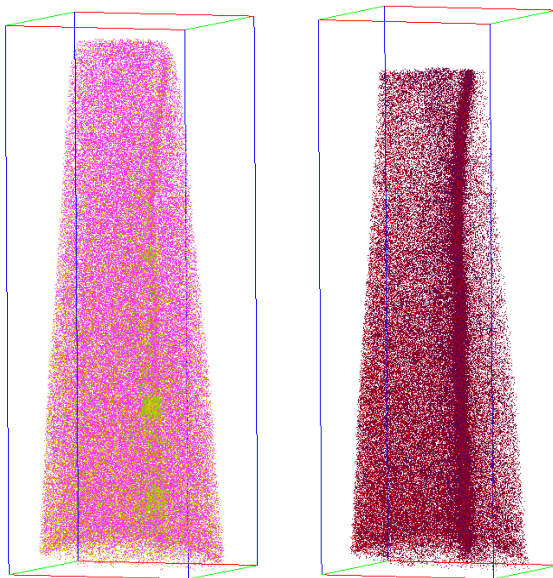
# EFFECT OF IRRADIATION ON GRAIN BOUNDARY CHEMISTRY IN FERRITIC STEELS

R.S. Mathew<sup>1</sup>, G.S. Was<sup>2</sup>, E.A. Marquis<sup>1</sup>

<sup>1</sup>Department of Material Science and Engineering, University of Michigan

<sup>2</sup>Department of Nuclear Engineering and Radiological Sciences, University of Michigan

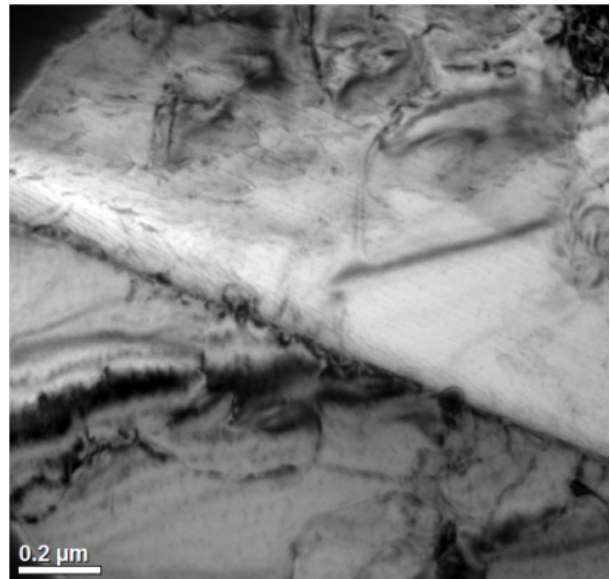
Ferritic-martensitic and high Cr ferritic steels have been receiving attention as potential candidates for nuclear applications such as pressure vessels in generation IV reactors, and as first walls in fusion reactors. One must have a thorough understanding of the microstructure of these alloys and their evolution under irradiation for safe long term use in nuclear reactors. Radiation induced segregation has raised significant interest due to its role in IASCC and corrosion of structural materials. Radiation induced depletion of chromium has been well established due to Cr being an oversized atom in austenitic stainless steels but its behavior in ferritic steels is not as clear. This work focuses on providing a systematic experimental database on the irradiation effects on ferritic steels based on dose, temperature and nature of the microstructure before and after irradiation. Ion irradiations have been performed on samples with Cr concentrations in the range of 5 to 15 wt% using 5MeV Fe<sup>++</sup> at a damage rate of 10<sup>-3</sup> dpa/s at temperatures between 200 and 600°C and to doses ranging from 0.1 to 100 dpa. Atom probe and TEM specimens have been made using Focused Ion Beam liftout technique on grain boundaries. Preliminary results on random high angle boundaries indicate enrichment of chromium and carbon at the grain boundary which increases with depth. This can be attributed to the increasing RIS with depth since the damage increases with depth. Nano sized nitride clusters can be observed to segregate along the grain boundary in 5Cr sample. Future work involves correlation of grain boundary character like the misorientation angle with the segregation observed.



Cr with nitrogen clusters

Carbon

APT atomic mapping near a grain boundary in a Fe5%Cr alloy



TEM bright field image of a grain boundary in a Fe5%Cr alloy

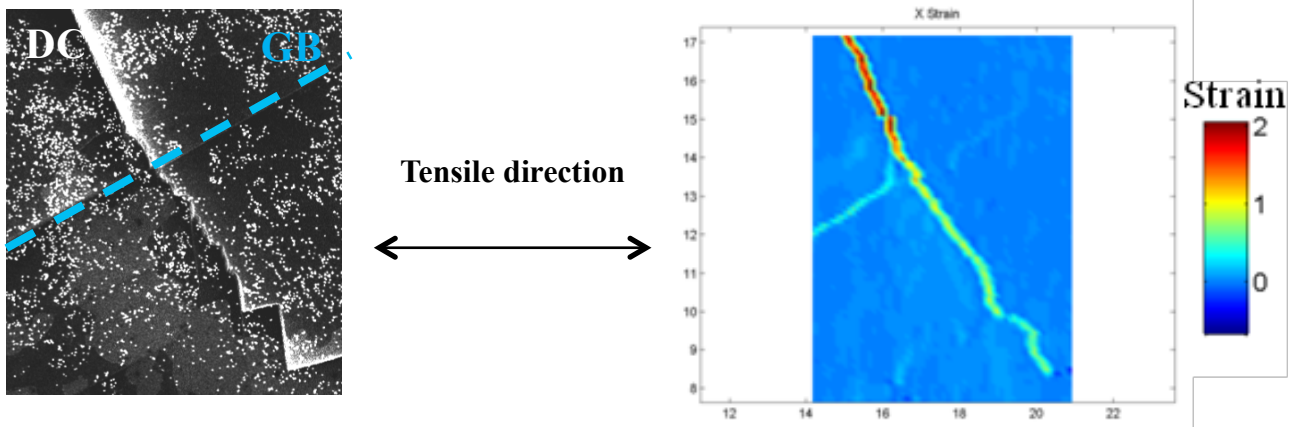
# LOCALIZED DEFORMATION AND INTERGRANULAR FRACTURE OF IRRADIATED ALLOYS UNDER EXTREME ENVIRONMENTAL CONDITIONS

M. D. McMurtrey, G. S. Was, I. M. Robertson, D. Farkas  
Department of Nuclear Engineering and Radiological Sciences, University of Michigan  
Department of Materials Science and Engineering, University of Illinois, Urbana Champaign  
Department of Materials Science and Engineering, Virginia Tech University

The goal of this project is to determine the role of localized deformation in austenitic steel during irradiation assisted stress corrosion cracking (IASCC). The project is a collaboration between UM, UIUC and Va Tech with the purpose of obtaining better understanding of the mechanisms involved in IASCC. Atomistic models of the experiments are being developed by Dr. Farkas' group at Virginia Tech University, and irradiated samples will be strained *in-situ* in a TEM by Dr. Robertson's group at the University of Illinois. Samples are being irradiated at the University of Michigan to study the cracking behavior and also to prepare samples for the *in-situ* TEM work to be performed at Illinois.

This year, a set of samples have been irradiated using 3 MeV protons in the Tandem Accelerator located in the Michigan Ion Beam Laboratory. Tensile samples from this irradiation will be used to quantify deformation within dislocation channels, which will be related to cracking. Sample surfaces will be coated in gold nano-particles, which will be imaged in an SEM prior to straining. Once the nano-particles are imaged, the samples will be strained in high temperature argon (288°C), and the nano-particles will be imaged again, to determine the amount of displacement caused by the deformation. Confocal microscopy will also be used to determine displacement normal to the sample surface. Following displacement measurements, the residual elastic strain will be analyzed using high resolution EBSD analysis. Once strain has been fully characterized, the samples will be strained further in water, and cracking behavior will be characterized, with respect to the known strain levels in the dislocation channel/grain boundary intersections.

This research has been supported by the Basic Energy Science office of the U.S. Department of Energy under grant DE-FG02-08ER46525.



SEM image of a grain boundary (light blue) and dislocation channel intersection (left), and map of the same area depicting the plastic strain in the horizontal direction (b). Strain is observed in the dislocation channel, as well as within the grain boundary.

# ACCELERATED STRESS CORROSION CRACK INITIATION OF ALLOYS 690 AND 600

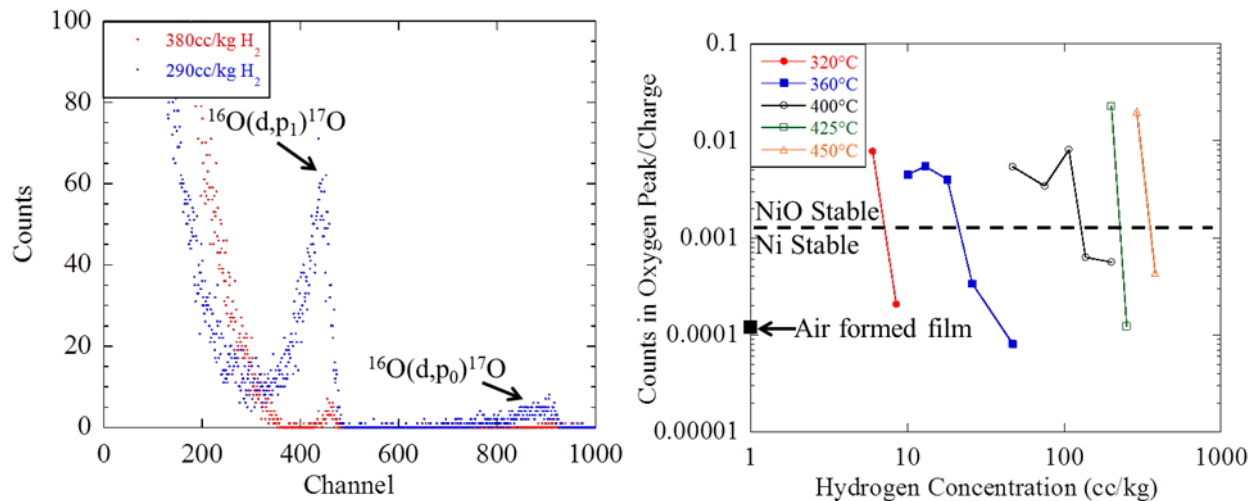
T. Moss, G.S. Was, University of Michigan

Department of Nuclear Engineering and Radiological Sciences, University of Michigan

In this project, stress corrosion crack (SCC) initiation susceptibility of alloys 690 and 600 is studied. At normal operating temperatures, little to no cracking is observed in alloy 690. To study the SCC behavior, the cracking must be accelerated which can be achieved by increasing the test temperature. However, the normal testing temperature of 360°C is already very close to the supercritical point (374°C), so accelerated tests will need to be conducted in the supercritical regime. There is some question as to whether the cracking mechanism in supercritical water is the same as in subcritical water. In order to determine if there is a mechanism change, tensile samples of alloys 690 and 600 are strained in a constant extension rate tensile (CERT) test and the amount of cracking is measured between 320°C and 450°C at a constant distance away from the Ni/NiO boundary. The amount of cracking is used to calculate the activation energy for crack initiation.

When measuring an activation energy, all external variables need to remain constant except for the temperature. In order to keep the corrosion environment the same, the environment must be modified to follow the Ni/NiO boundary as the temperature is changed. However, the location of the Ni/NiO boundary in terms of the amount of dissolved hydrogen was not known in supercritical water. Samples of pure nickel were exposed for 72 hours at temperatures between 320°C and 450°C and varying concentrations of dissolved hydrogen. The location of the boundary was determined by analyzing the nickel samples to see if oxygen was present on the surface, indicating an oxide had formed. To measure the oxide thickness, nuclear reaction analysis (NRA) was performed using an 850 keV  $D^+$  beam to measure the protons from the  $^{16}O(d,p_1)^{17}O$  reaction as shown in Figure 1a. To determine how much of an oxide formed, a ratio was taken between the number of counts in the  $^{16}O(d,p_1)^{17}O$  peak and the integrated charge for each condition as shown in Figure 1b. The NRA analysis was vital in determining quantitatively what cracking environment to use for SCC experiments.

This research is supported by EPRI Contract #EP-P35621.



Example of NRA data taken from two samples tested at 450°C with 380 and 290cc/kg dissolved hydrogen (left), and oxygen content on the surface of Ni coupons as a function of temperature and dissolved hydrogen concentration (right).

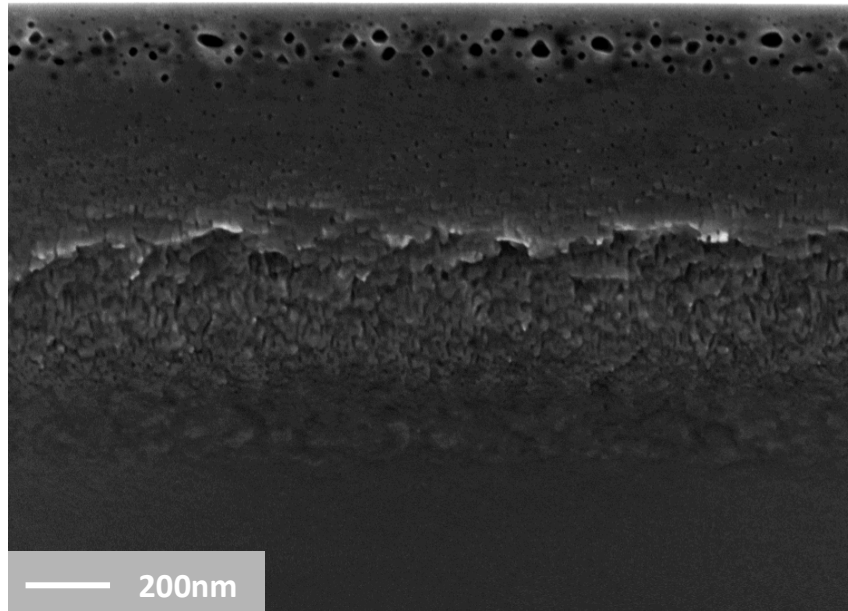
# HIGH DOSE OXYGEN IMPLANTATION OF GERMANIUM FOR THE DEVELOPMENT OF ANTI-REFLECTIVE COATINGS

A. Swisher, A. Pogrebnyakov, T. Mayer  
Department of Electrical Engineering, Pennsylvania State University

Ion implantation provides a unique method for direct tailoring of the optical properties of a material system. High dose oxygen implantation performed on a crystalline germanium substrate has been shown to be a promising process for fabricating low loss anti-reflective coatings. Heavy ion irradiation can result in the formation of  $\text{GeO}_x$  in the near surface implanted regions. The refractive index of  $\text{GeO}_2$  in the ultraviolet and visible regions of the electromagnetic spectrum is  $\sim 1.75$ , allowing for significant reduction in the reflectivity of the sample.

Single crystal undoped Ge wafers were implanted with oxygen doses ranging from  $1 \times 10^{14}$  to  $2 \times 10^{18} \text{ cm}^{-2}$  at 300 keV, with the substrate temperature held at a constant  $400^\circ\text{C}$ . Ellipsometry measurements of the samples indicate a significant reduction in the refractive index in the UV, visible and near-IR regions after implantation, indicating the formation of a substoichiometric germanium oxide layer. In addition, an electron microscopy examination shows a morphology change in the substrate corresponding to the implanted region.

This research is supported by Materials Research Science and Engineering Center (MRSEC)



FESEM image of Ge substrate which has been implanted with  $2 \times 10^{18} \text{ cm}^{-2}$  at 300keV. A buried  $\text{GeO}_x$  layer is formed 500nm below the substrate surface, with noticeable void formation within the top 100nm.

# THE BEHAVIOUR OF BINARY Zr-Sn ALLOYS UNDER PROTON IRRADIATION

M. Preuss, A. Harte and T. Seymour  
School of Materials, University of Manchester, UK

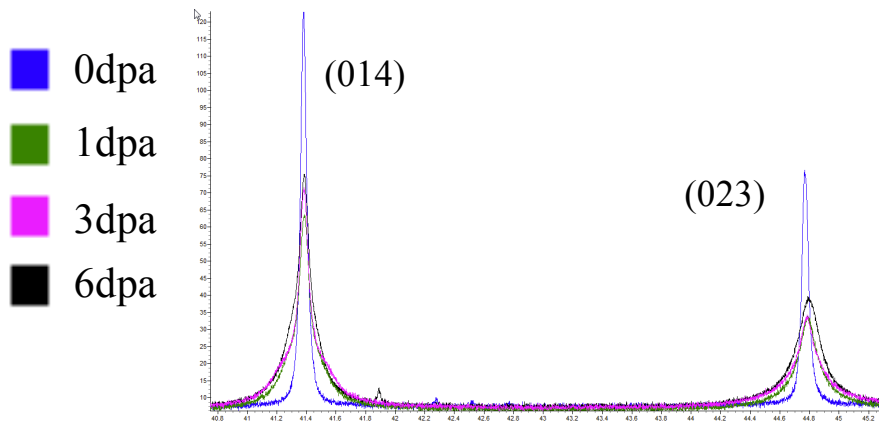
Zirconium (Zr) alloys are utilised for the cladding and structural components of PWR and BWR cores, due to their mechanical and corrosion properties at operating conditions and their low neutron absorption cross section. The deformation behaviour of Zr alloys under irradiation is therefore of considerable interest.

A significant aspect of the behaviour's complexity is the effect of alloying on the microchemical and microstructural behaviour. It is the purpose of this and future research within the group to irradiate model binary alloys with protons and ions. This will reduce the complexity of studying defect behaviour in Zr alloys and result in the elucidation of the role of the various alloying and impurity elements in neutron-irradiated material.

In the present study, recrystallised binary Zr-Sn alloys with varying concentrations of Sn were irradiated to low dose (1, 3, and 6 dpa) at  $\sim 350^\circ\text{C}$  with 2 MeV protons at an approximate dose rate of  $0.08 \text{ dpa s}^{-1}$ .

Reflecting angle synchrotron XRD has been performed at the Diamond Light Source in the UK and preliminary results indicate the presence of irradiation-induced dislocations through distinctive peak broadening, and perhaps the existence of precipitates introduced during irradiation, although this has not been confirmed. Further analysis using diffraction peak broadening software developed by Ribárik, Ungár and Gubicza (2001) will be implemented in the near future in order to study the evolution of dislocation density and arrangement.

Complementary analysis will be performed by FEG (S)TEM at the University of Manchester. The aim of such microscopy will be to corroborate the conclusions of the synchrotron XRD data and to elucidate the role of alloying and impurity elements in such changes *via* EDX.



The (014) and (023) peaks of the Zr-0.15% wt. Sn alloy in unirradiated and irradiated states at 1, 3 and 6 dpa at log scale. Peak broadening with irradiation is clearly observed. Small peaks just visible to the right of the (014) peak could possibly be attributed to secondary phase particles.

# IRRADIATION ACCELERATED CORROSION OF REACTOR CORE MATERIALS

S. S. Raiman<sup>1</sup>, P. Wang<sup>1</sup>, Z. Jiao<sup>1</sup>, G. S. Was<sup>1</sup>, D.M. Bartels<sup>2</sup>, J. Jacob<sup>2</sup>

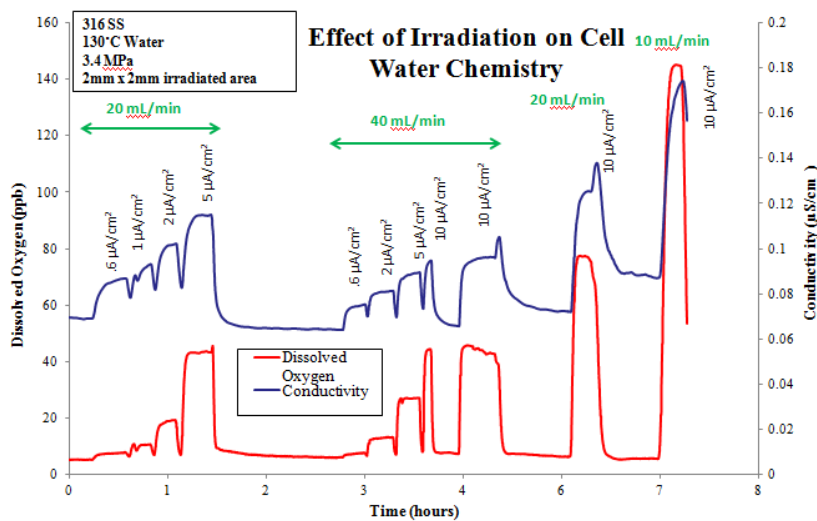
<sup>1</sup>Department of Nuclear Engineering and Radiological Sciences, University of Michigan

<sup>2</sup>University of Notre Dame Radiation Laboratory

The goal of this project is to understand the mechanisms behind irradiation accelerated corrosion (IAC). It has been shown that irradiation causes order-of-magnitude increases in corrosion growth rate, which is a serious problem in reactor cores. Three mechanisms have been identified, which are believed to be the main drivers of IAC. By properly understanding their roles, better models can be developed, and accurate predictions can be made when considering license extensions for existing light-water reactors.

The first effect, radiolysis, affects corrosion by creating oxidizing species in coolant water, raising the corrosion potential. Secondly, radiation induces exciton production in the materials which can affect corrosion kinetics. Lastly, displacement damage produces defects which increase diffusion rates.

The experiment at the Michigan Ion Beam Lab will be testing all three effects, while collaborators at The University of Notre Dame perform experiments to isolate one or two of the effects. A new, dedicated beamline has been built especially for this project. A corrosion cell containing 320°C, 1800psi water is fixed at its end. Samples serve as the barrier between the high vacuum beamline and the corrosion cell. Carefully designed safety systems protect beamline and accelerator components in the event of sample failure. In-Situ diagnostics give real-time measurements of dissolved oxygen production and ECP. Initial results show a large increase in oxygen production with irradiation. Oxygen production is a product of radiolysis in water, and is suspected to be a cause of irradiation accelerated corrosion.



This research is supported by the U.S. Department of Energy and Electricite de France

At left is a plot of oxygen production in water due to proton irradiation. Oxygen production is a product of radiolysis in water, and is suspected to be a cause of irradiation accelerated corrosion.

Increases in beam current at 130°C are accompanied by increases in oxygen content of water at the cell outlet and also an increase in the conductivity.

# ZnSnN<sub>2</sub>: A NEW EARTH-ABUNDANT ELEMENT SEMICONDUCTOR FOR SOLAR CELLS

N.A. Feldberg<sup>a</sup>, G. Vardar<sup>b</sup>, J.D. Aldous<sup>a</sup>, R.S. Goldman<sup>b</sup> and S.M. Durbin<sup>a,c</sup>

<sup>a</sup> Department of Physics, University at Buffalo

<sup>b</sup> Department of Materials Science and Engineering, University of Michigan,

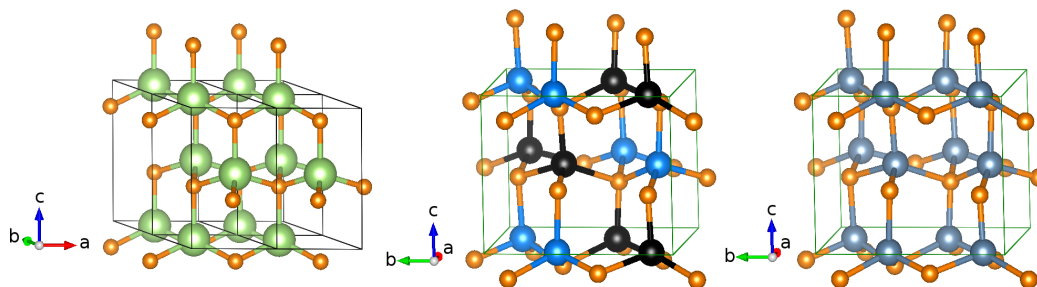
<sup>c</sup> Department of Electrical Engineering, University at Buffalo

For more than two decades, the search has been on to find a semiconducting material with the potential to replace silicon as a photovoltaic material. Cu(In,Ga)Se<sub>2</sub> (CIGS) was an early candidate and is currently one of the most cost-competitive materials, with a reported peak efficiency of 20.3% for a multijunction cell. InGaN has a direct band gap tunable across the whole solar spectrum making it an obvious and enticing candidate. However, both materials suffer from fundamental limitations. For example there is difficulty in doping CIGS n-type and InGaN p-type, with unintentional doping being a serious issue, while a surface electron accumulation layer on all surfaces of In-rich InGaN makes it difficult to form p-n junctions. Moreover, both CIGS and InGaN contain In and Ga, elements which are not hugely abundant and comparatively expensive, with almost no reclamation activity for either metal.

More recently, the family of Zn-IV-N<sub>2</sub> has been predicted to offer many of the same properties as InGaN, except using elements which are extremely abundant in the earth's crust and subject to widespread recycling activity. Currently, the Ge and Si containing members of this family have been synthesized and investigated in some detail. However, ZnSnN<sub>2</sub> remains a relative unknown.

One of the interesting observations from the work on the Ge and Si containing compounds is the apparent discrepancy between the predicted and observed crystal structure. The DFT predicted structure of the Zn-IV-N<sub>2</sub> compounds is orthorhombic (space group Pna2<sub>1</sub>), closely related to the wurtzite structure of the III-N (Fig. 2(a) and (b)). The structure is obtained by substituting Ga for alternating Zn and group IV elements, with a slight distortion of the lattice induced as a result of different Zn-N and IV-N bond lengths. However, to date, the majority of the samples grown from within this family show in x-ray diffraction studies a wurtzitic or monoclinic structure (space group P2<sub>1</sub>). This discrepancy between expected and observed crystal structure is thought to be the result of the cation sublattices being randomly ordered (Fig. 2(c)), which in XRD would give the appearance of increased symmetry. To date, little direct experimental evidence exists which confirms this.

Rutherford back scattering spectrometry (RBS) confirmed that achieving proper stoichiometry requires careful tuning of the growth parameters and a significant overpressure of zinc; initial films were Sn-rich and in some cases tin droplets could be observed. Subsequently, adjusting the metal flux ratio based on RBS results, led to single crystal film growth. All films, however, exhibit a monoclinic structure, consistent with sublattice disorder, with no evidence for an orthorhombic phase – even for nominally stoichiometric films.



Crystal structures of (a) GaN, (b) orthorhombic Zn-IV-N<sub>2</sub>, and (c) monoclinic Zn-IV-N<sub>2</sub>.

# BISMUTH INCORPORATION IN GaAsBi FILMS GROWN BY MOLECULAR BEAM EPITAXY

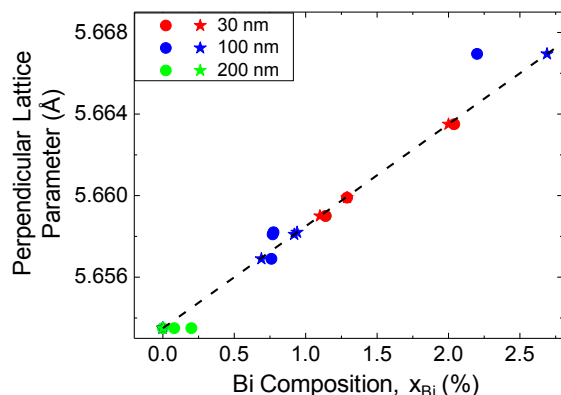
G. Vardar<sup>1</sup>, R. L. Field III<sup>2</sup>, M. V. Warren<sup>1</sup>, M. Kang<sup>1</sup>, S. Jeon<sup>1</sup>, R. S. Goldman<sup>1,2</sup>

<sup>1</sup>Department of Materials Science and Engineering, University of Michigan

<sup>2</sup>Department of Physics, University of Michigan

Due to their significant energy band gap bowing, dilute bismide compound semiconductor alloys can be grown with a range of band gap energies while maintaining near lattice matching with common substrates. Thus, the alloys are promising candidates for a wide range of applications, including long-wavelength light-emitters and detectors, high-performance electronic devices, and high efficiency solar cells. Although a narrow range of system-dependent As-to-Ga flux ratios have been reported to enable GaAsBi film formation, a detailed understanding of the influences of system-independent growth parameters remains unknown. Therefore, we have investigated the influence of As<sub>2</sub>:Ga beam equivalent pressure (BEP) ratio, Bi:As<sub>2</sub> BEP ratio, and growth rate on the Bi incorporation mechanisms in GaAsBi alloy films. For our studies, we grow GaAsBi alloy films by molecular beam epitaxy (MBE). To estimate the bismuth content in the films, we use a combination of high-resolution x-ray diffraction (HRXRD) and Rutherford backscattering spectroscopy (RBS). The HRXRD data allows us to determine the strain of the GaAsBi layer with respect to the GaAs substrate. (To date, the synthesis of GaBi has not been reported; therefore, the GaBi crystal structure and lattice parameters based upon density functional theory are typically used to interpret x-ray diffraction data [1].) The strain calculated from HRXRD is then used to calculate the Bi content of the GaAsBi layer assuming that the lattice constant of GaAsBi varies linearly with increasing Bi content [2]. For all GaAsBi films, HRXRD scans are simulated with Bede RADS software and the bismuth content is adjusted to match the HRXRD data. For comparison, we use RBS to determine the bismuth content of the GaAsBi films. The backscattered spectra for channel-to-energy conversions are simulated with SIMNRA [3] and the bismuth content and film thickness are adjusted to match the RBS data. For most GaAsBi films, the agreement between HRXRD and RBS determination of Bi composition is within 15% (Figure). Vertically inhomogeneous Bi incorporation in >100nm thick GaAsBi layers is likely contributing to the discrepancy between HRXRD and RBS determinations of Bi composition [4].

We gratefully acknowledge the support of the National Science Foundation through Grant DMR-1006835. G. V. acknowledges the support of the Fulbright Foreign Student Fellowship.



Perpendicular lattice parameter as a function of bismuth composition ( $x_{Bi}$ ), as determined by HRXRD (stars) and RBS (circles). 30 nm, 100 nm, 200 nm GaAsBi films are represented by red, blue, and green.

# DETERMINING THE MECHANISM OF RADIATION-INDUCED SEGREGATION IN FERRITIC-MARTENSITIC ALLOYS

J.P. Wharry, G.S. Was

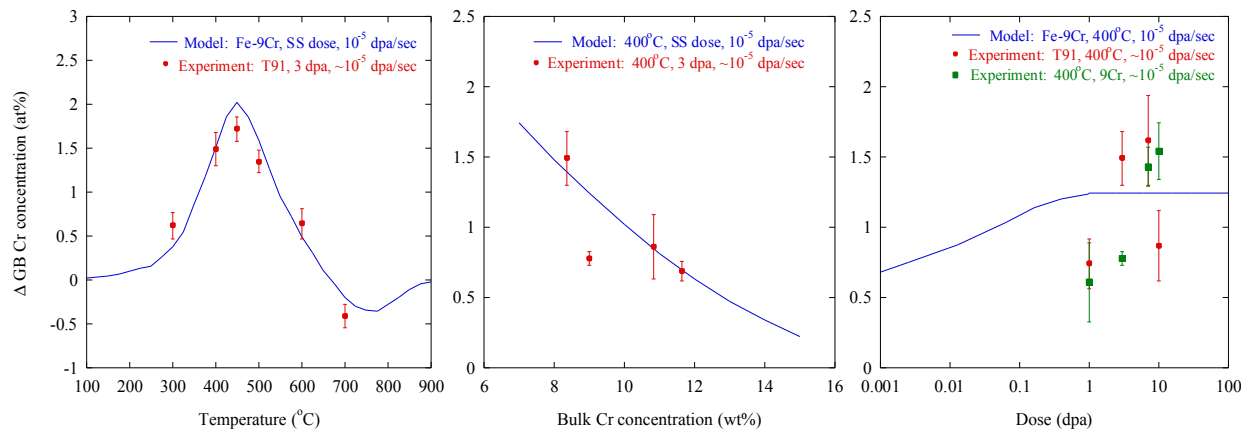
Department of Nuclear Engineering & Radiological Sciences, University of Michigan

Radiation-induced segregation (RIS) is a non-equilibrium process by which alloying elements segregate toward or away from grain boundaries under irradiation. Ferritic-martensitic (F-M) alloys, which are candidates for structural and cladding components in advanced fast reactors, could be susceptible to RIS of Cr, which could cause embrittlement and degradation of materials properties. Prior to this study, there was limited understanding of the behavior of Cr RIS in F-M alloys, and the mechanism of this RIS was unknown.

This study systematically evaluated the behavior of Cr RIS as a function of irradiation temperature, bulk Cr composition of the alloy, and irradiation dose. Irradiations were conducted over a temperature range 300-700°C, dose range 1-10 dpa, using 2.0 MeV protons. The alloys studied were T91 (8.37 wt%Cr), HT9 (11.63 wt%Cr), HCM12A (10.83 wt%Cr), and an Fe-9Cr model alloy. In all but one condition, Cr enriched at grain boundaries. The temperature dependence of RIS exhibited a bell-shaped curve of Cr enrichment, with a switch from Cr enrichment to Cr depletion between 600°C and 700°C. The dependence of RIS on bulk Cr content exhibited a negative slope. The dependence of RIS on dose was minimal, with an increase in the amount of RIS up to ~7 dpa, followed by either a steady-state (as observed in the Fe-9Cr model alloy) or a decrease in the amount of Cr enrichment (as observed in T91).

A model of the Inverse Kirkendall (IK) mechanism has calculated RIS behaviors comparable to those observed experimentally, as seen in the figures below. The IK model calculated the bell-shaped temperature dependence, decreasing amount of Cr RIS with increasing bulk Cr content, and the steady-state behavior of RIS as a function of dose. Most notably, however, the IK model calculated the change from Cr enrichment to Cr depletion between 600°C and 700°C, because of the intersection of the Cr to Fe diffusion coefficient ratio for interstitials with that for vacancies. A model of the alternative solute drag mechanism was unable to calculate the change from Cr enrichment to Cr depletion. This work concluded that Cr RIS in F-M alloys is consistent with the IK mechanism.

This work is supported by the U.S. Department of Energy under grant DE-AC07-05ID14517.



Experimental measurements (points) and IK model calculations (lines) of the change in grain boundary Cr concentration as a function of temperature (left), bulk Cr concentration (middle), and dose (right).

# AN EXPERIMENTAL TECHNIQUE FOR VERY HIGH TEMPERATURE PROTON IRRADIATIONS

J.P. Wharry, G.S. Was

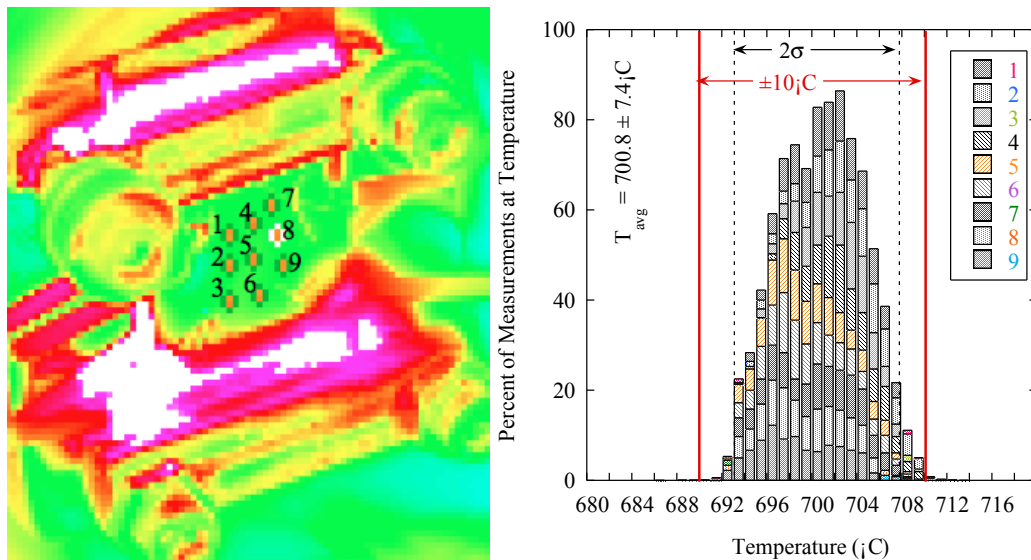
Department of Nuclear Engineering & Radiological Sciences, University of Michigan

Historically, proton irradiations at the Michigan Ion Beam Laboratory were limited to temperatures of  $\leq 600^\circ\text{C}$ . Above these temperatures, the vapor pressure of tin and indium inhibit their use as a heat transfer medium between the irradiated sample(s) and the stage. But to reach higher irradiation temperatures, it became necessary to investigate alternative techniques to provide efficient and even heat transfer between the sample and the stage. This work is the proof of concept of a pyrolytic graphite sheet for heat transfer for  $\geq 600^\circ\text{C}$  proton irradiations.

A single layer of 0.1 mm high thermal conductivity pyrolytic graphite sheet (PGS) was compressed between a plate specimen of ferritic-martensitic alloy T91 and the polished Ni irradiation stage. The PGS is a highly oriented graphite polymer film; its flexibility allows it to pack into the surface roughness of the specimen and the stage, mimicking the “wetting” effect of liquid metal. Prior to irradiation, the evenness of the heat transfer across the PGS was confirmed with an array of eight thermocouples. For the irradiation, four thermocouples were used to calibrate the two-dimensional infrared thermal image, which was used throughout the irradiation to monitor and record temperatures.

The T91 plate with PGS sheet for heat transfer was irradiated to 3 dpa at a target temperature of  $700^\circ\text{C}$  using 2.0 MeV protons. Nine areas of interest were set up within the irradiated region, as shown in the thermal image (left). The thermal image also illustrates even beam heating across the T91 plate. Temperature control of this irradiation was consistent with conventional indium- or tin-backed proton irradiations: the average temperature of all nine areas of interest was  $700.8 \pm 7.4^\circ\text{C}$ . Thus, a sheet of PGS is confirmed to provide efficient and even heat transfer for proton irradiations exceeding  $600^\circ\text{C}$ .

This work is supported by the U.S. Department of Energy under grant DE-AC07-05ID14517.



2-D infrared thermal image of T91 plate with PGS for heat transfer, with nine areas of interest identified (left). Temperature histogram T91 plate, from  $700^\circ\text{C}$ , 3 dpa irradiation with 2.0 MeV protons (right).

# PROBING THE CHEMICAL COMPOSITION OF ANNEALED AMORPHOUS INDIUM-GALLIUM-ZINC-OXIDE THIN FILMS

E. K. Yu<sup>1</sup>, F. Naab<sup>2</sup>, G. Baek<sup>1</sup>, and J. Kanicki<sup>1</sup>

<sup>1</sup>Department of Electrical Engineering and Computer Science, University of Michigan

<sup>2</sup>Department of Nuclear Engineering and Radiological Sciences, University of Michigan

The amorphous oxide semiconductor In-Ga-Zn-O (a-IGZO) thin-film transistor (TFT) was first fabricated in 2004 by Nomura *et al.* and has since been the focus of intense research efforts. The a-IGZO TFT has several significant advantages: a-IGZO has high electron mobility (typically  $\sim 10\text{cm}^2/\text{Vs}$ ) and can be uniformly deposited over a large area in its amorphous phase, making it a prime candidate for next-generation large-size ultra-high definition 4K AM-LCD and AM-OLED displays. It also has very low leakage current ( $\sim 10^{-14}\text{A}$ ) and is particularly attractive for low-power mobile displays.

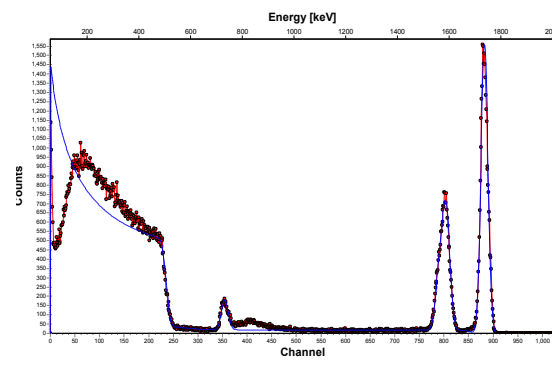
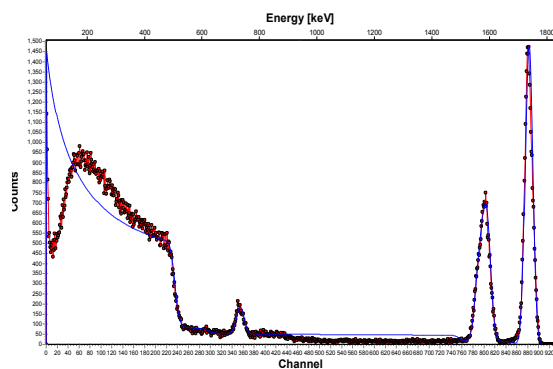
We are working on optimizing the fabrication process for a-IGZO TFTs in the Michigan LNF cleanroom using RF and DC sputtering to improve two key TFT parameters: the sub-threshold slope and the threshold voltage. Post-deposition annealing at around 300C is an important step during the TFT fabrication process. However, there are no clear answers as to what happens to the IGZO channel layer during annealing. With assistance from the Michigan Ion Beam Laboratory (MIBL), we hope to shed some light on the IGZO microstructure changes during annealing using Rutherford Backscattering (RBS). By comparing the RBS signal of two IGZO thin films deposited on a smooth carbon plate – one film as deposited and the other annealed – we can verify that the IGZO film composition does indeed change during annealing in that the oxygen content of the film increased noticeably. The oxygen content is related to oxygen vacancies in the a-IGZO film and is the direct source of charge carriers in the oxide semiconductor. The work done in the MIBL has yielded some very useful and insightful information for our project.

Film composition before annealing:

In:Ga:Zn:O = 1.10 : 1.04 : 0.91 : 3.95

Film composition after annealing:

In:Ga:Zn:O = 1.01 : 0.96 : 0.76 : 4.27



RBS plots of In:Ga:Zn:O thin film of stoichiometry 1.101:1.04:0.91:3.95 before annealing (left) and 1.01 : 0.96 : 0.76 : 4.27 after annealing (right).

# ROLE OF MICROSTRUCTURE ON Ag TRANSPORT IN SiC

## ATR-NSUF PROJECT

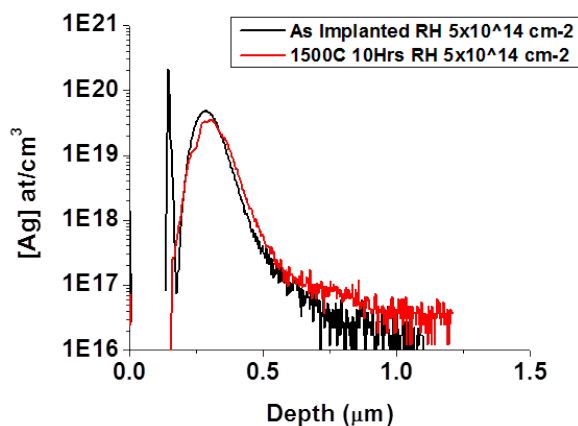
T. Gerczak, I. Szlufarska

Department of Materials Science and Engineering, University of Wisconsin-Madison

In this work, silicon carbide (SiC) substrates have been implanted with  $\text{Ag}^+$  ions to fabricate ion implantation diffusion couples. The work is focused on understanding transport mechanisms of Ag in SiC to gain insight on Ag release observed in the novel tristructural isotropic (TRISO) fuel form which is under development to support the advancement of the Very High Temperature Reactor concept. Currently, there are competing hypotheses on which phenomenon is responsible for release and the goal of this work is to directly measure Ag diffusion in polycrystalline SiC.

The current study builds off of previous experiments which imply impurity diffusion to be active in the polycrystalline CVD-SiC system at  $1500^\circ\text{C}$ , as shown in the Figure. Markers of impurity diffusion are suggested by the extension of the Ag concentration further into the bulk after exposure at high temperature. To further examine the Ag/SiC system, additional ion implantation diffusion couples have been fabricated by implantation, polycrystalline CVD-SiC and single crystal 4H-SiC substrates, with 400 kV  $\text{Ag}^+$  to fluences of  $1 \times 10^{14}$  and  $5 \times 10^{14}$   $\#/\text{cm}^2$  at  $300^\circ\text{C}$ . The inclusion of the single crystal samples in the study will serve to isolate lattice diffusion contributions, while the polycrystalline CVD-SiC allows for insight on grain boundary contributions. The expanded study will investigate diffusion at elevated temperatures and conditions building off of previous experimental observations. Additional conditions will illuminate the kinetics of diffusion and allow insight on the potential for Ag diffusion being the responsible mechanism for Ag release from TRISO fuel. Samples are currently being prepared for thermal exposure.

This research is being performed using funding from the DOE Office of Nuclear Energy's Nuclear Energy University Programs. NEUP Grant #00118099



Secondary ion mass spectroscopy depth profile of Ag in CVD-SiC substrate with 200 nm diamond-like-carbon cap, demonstrating extension of Ag concentration into bulk after  $1500^\circ\text{C}$  10 Hour thermal exposure, indicative of thermal diffusion.

# IRRADIATION DAMAGE AND LOCALIZED DEFORMATION OF AUSTENITIC STAINLESS STEELS IN PWR ENVIRONMENT

M. Le Millier<sup>1</sup>, J. Crépin<sup>1</sup>, C. Duhamel<sup>1</sup>, F. Gaslain<sup>1</sup>, A. Pineau<sup>1</sup>, O. Calonne<sup>2</sup>, L. Fournier<sup>2</sup>, Y. Vidalenc<sup>2</sup>, E. Heripre<sup>3</sup>, O. Toader<sup>4</sup>

<sup>1</sup>Centre des Matériaux, CNRS UMR 7633, Mines ParisTech, France

<sup>2</sup>AREVA NP, France

<sup>3</sup>Laboratoire de Mécanique des Solides, CNRS UMR 7649, Polytechnique-X-Mines ParisTech, France

<sup>4</sup>Michigan Ion Beam laboratory, University of Michigan

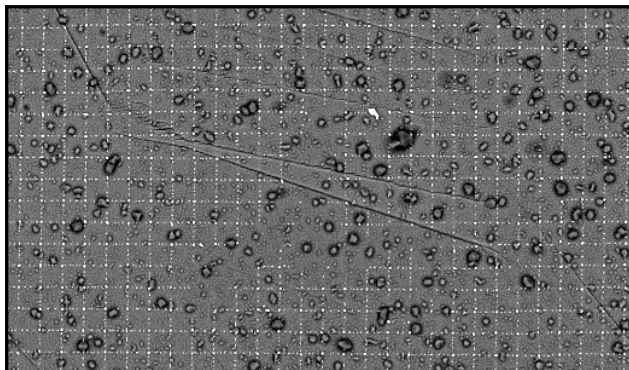
The purpose of this work is to determine initiation criteria for IASCC that take into account radiation dose, microstructural parameters of the alloy and quantitative mechanical data on the localized deformation.

To reach this goal, a protocol is developed to correlate crack initiation and propagation to crystallographic orientations and strain field measurements by using SEM digital imaging correlation technique coupled with EBSD cartography. Thereby, 304L specimens were irradiated with 2 MeV protons at 360°C to 5 and 10 dpa. Those specimens are strained to various macroscopic strains in PWR simulated primary water. We observe intergranular cracks, which occurred on random high angle boundaries, perpendicular to the tensile axis. The strain field analysis shows a strong heterogeneity, with localization near some grain boundaries for the irradiated areas. Quantitative data obtained are also compared with those obtained with non-irradiated samples.

This research is supported by the chair AREVA of Mines ParisTech graduate school.

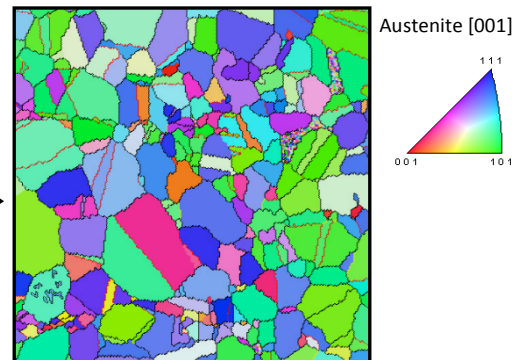
## Sample irradiated to 5 dpa and strained to 1% in simulated primary water

Cracking and oxidation features, characterization of slip lines



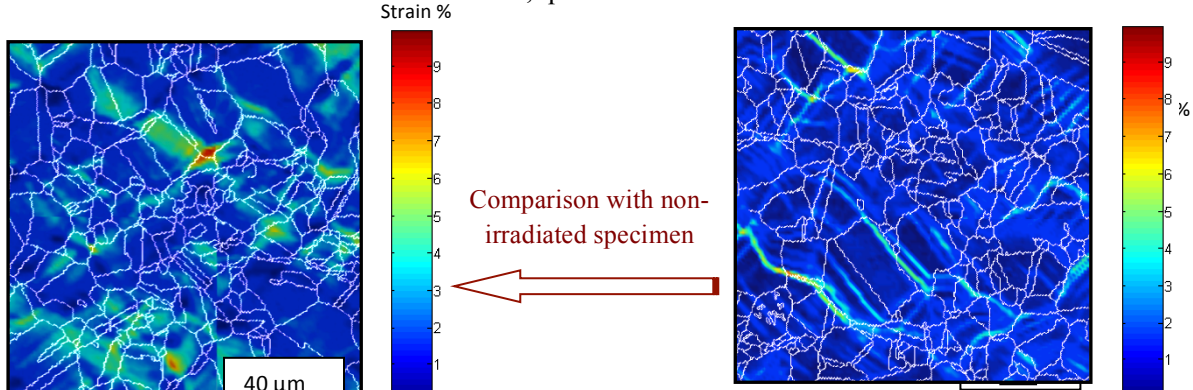
SEM image (BSE) on the irradiated area

Microstructure and crystallographic orientations map



EBSD map of the global area

Strain field measurements, quantitative data on localized deformation



Von Mises equivalent strain field ( $200 \times 200 \mu\text{m}^2$  with  $4 \mu\text{m}$  gauge length for a non-irradiated sample

Von Mises equivalent strain field ( $200 \times 200 \mu\text{m}^2$  with  $4 \mu\text{m}$  gauge length for a irradiated sample

# STUDY OF IODINE-INDUCED STRESS CORROSION CRACKING OF ZIRCONIUM ALLOYS, INFLUENCE OF IRRADIATION AND STRESS BIAXIALITY

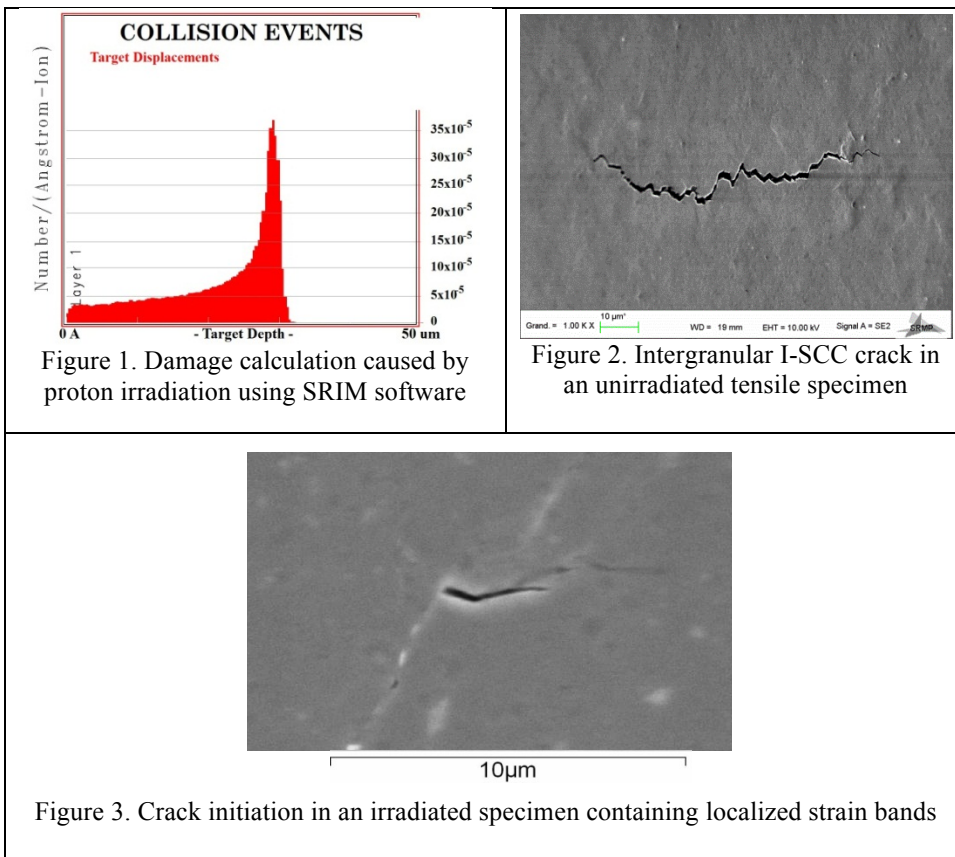
Mozzani N.<sup>1,2</sup>, Andrieu E.<sup>2</sup>, Auzoux Q.<sup>1</sup>, Blanc C.<sup>2</sup>, Leboulch D.<sup>1</sup>

<sup>1</sup>Commissariat à l’Energie Atomique; CEA Saclay, DMN/SEMI/LCMI; France

<sup>2</sup>CIRIMAT/ENSIACET, Université de Toulouse, France

During power transients in nuclear reactors, fuel cladding may fail due to the pellet-cladding interaction (PCI). The mechanism involved is iodine-induced stress corrosion cracking (I-SCC). I-SCC can be observed in laboratory and notably when testing cladding material in iodized methanol at room temperature. Neutron irradiation leads to a higher sensitivity to I-SCC and several studies showed the similarities between proton and neutron irradiation concerning changes of microstructures.

In this study, tensile specimens of fully recrystallized Zircaloy-4 are extracted from thin sheets (0.5 mm thickness). The cracking domain of unirradiated Zircaloy-4 has been thoroughly studied and boundaries are now known in terms of iodine concentration, strain rates and threshold plastic strain. Proton irradiations were carried out in a plate of the material. SRIM calculations showed that for proton energy of 2 MeV, Bragg’s peak is located at a depth of 30  $\mu\text{m}$ . Irradiation conditions were chosen to obtain a dose of 2 dpa at 60% of the peak’s depth. The temperature was 350°C. The first tests on irradiated samples confirmed increased I-SCC sensitivity. A strain rate effect is still present in these samples, with a threshold plastic strain of 0.5% at  $10^{-4} \text{ s}^{-1}$  and of 1.5% at  $10^{-3} \text{ s}^{-1}$ , instead of 2% and 3% respectively for unirradiated specimens. Intergranular cracks seem to nucleate at the intersection of localized strain bands and grain boundaries.



# OPTIMIZATION OF H<sup>+</sup> IMPLANTATION PARAMETERS FOR EXFOLIATION OF 4H-SiC FILMS

V. P. Amarasinghe<sup>1,2,4</sup>, L. Wielunski<sup>1,3</sup>, A. Barcz<sup>5</sup>, L. C. Feldman<sup>1,2,3</sup>, G. K. Celler<sup>1,2</sup>

<sup>1</sup>Institute for Advanced Materials, Devices, and Nanotechnology (IAMDN)

<sup>2</sup>Department of Materials Science and Engineering, Rutgers University

<sup>3</sup>Department of Physics, Rutgers University

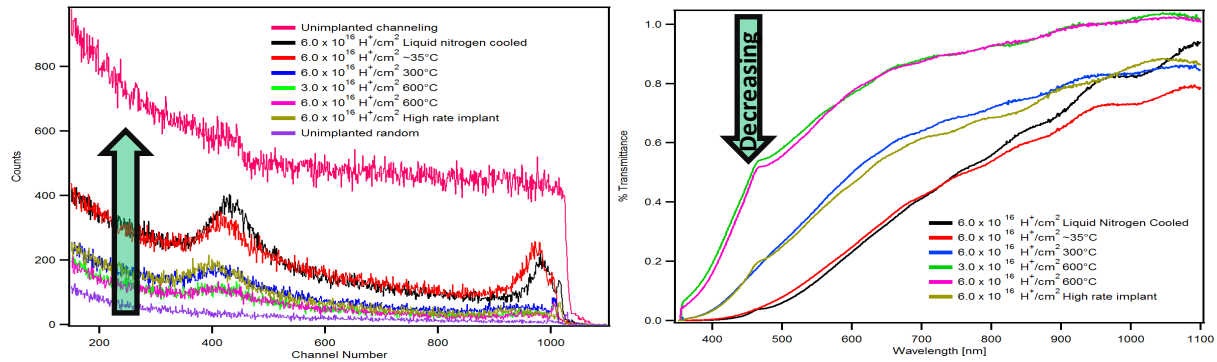
<sup>4</sup>Department of Chemistry, Rutgers University

<sup>5</sup>Institute of Electron Technology/Institute of Physics PAS, Warsaw, Poland.

Hydrogen ion implantation into single crystalline SiC with a dose of the order of  $5 \times 10^{16} \text{ cm}^{-2}$  can cause formation of nanovoids and microcracks under the surface, at a depth corresponding roughly to the projected implantation range  $R_p$  and, after a subsequent annealing at elevated temperatures, these defects lead to exfoliation (and with suitable preprocessing to layer transfer to a new substrate).

In this study we have investigated exfoliation of thin films of 4H-SiC under different implantation conditions. Implantation doses of  $3 \times 10^{16}$  and  $6 \times 10^{16} \text{ H}^+ \text{ cm}^{-2}$  and implant temperatures from 77K to 873K were employed to study surface blistering and exfoliation behavior. We have concentrated on 180 keV ion energies that lead to exfoliation of about 1  $\mu\text{m}$  thick films. To characterize damage distribution in implanted samples we utilized ion channeling with 2.4 MeV He ions (Figure), while SIMS spectra provided hydrogen depth profiles of selected samples. Optical transmittance in the 0.3-1.1  $\mu\text{m}$  spectral region (Figure) provides a simple means for evaluating depth-integrated lattice damage that increases with H<sup>+</sup> fluence. Research examining the influence of implant conditions on surface blistering and layer exfoliation is ongoing.

This work has been partially supported by the Semiconductor Research Corporation (SRC) through GRC task 2166.001.



Ion channeling data (left) and optical transmittance spectra (right) in thin films of 4H-SiC under different implantation conditions.

# HETEROJUNCTION-ASSISTED IMPACT IONIZATION: SiC EXPLORATION

J. Wang

Department of Materials Science, University of Illinois

This project combines thin film synthesis, analysis, and modeling expertise to develop heterojunction-assisted impact ionization (HAI) to achieve a quantum efficiency greater than 1 in unbiased semiconducting heterostructures and nanostructured thin films. HAI combines a narrow, indirect band gap host material with wide, direct or indirect gap absorbers (harvesters) in the form of thin films, nanorods, or nanoparticles. Higher energy photons generate carriers in the wide-gap material. As these pass into the narrow-gap material they can decay through impact ionization (II) to produce additional carriers. Achieving the desired increase in QE through HAI requires locating and optimizing host and harvester combinations and structures with appropriate band gaps, offsets, II rates, etc.

An approach to produce designed nanostructure is to implant crystalline Si with carbon and then anneal to recrystallize the Si and to permit the C to diffuse and to form SiC precipitates. This is possible because the solubility is low. The implant dose will determine the size of the precipitates, and the implant energy will determine their depth distribution.

In the lab, two possible combinations of harvester and host are proposed: SiC-harvester, C-host; CdS-harvester, CIGS-host.

The first combination was explored first. Ultra high purity carbon samples were implanted in the following conditions:

50keV to  $6 \times 16/\text{cm}^2$ ,  $6 \times 15/\text{cm}^2$ , and  $6 \times 14/\text{cm}^2$   
100keV to  $8 \times 16/\text{cm}^2$ ,  $8 \times 15/\text{cm}^2$  and  $8 \times 14/\text{cm}^2$   
150keV to  $1 \times 17/\text{cm}^2$ ,  $1 \times 16/\text{cm}^2$  and  $1 \times 15/\text{cm}^2$

After receiving the implanted samples, three different annealing processes, which are 1200°C:30min, 1100°C:60min, and 1100°C:30min, were done on each sample. X-ray diffractions under 45keV 40 mA were done on the samples to explore the silicon carbonate. However, no the silicon carbonate was found by looking at the XRD spectrum.

In the future, more techniques will be used to analyze the samples and to characterize the effects of the annealing process.

# SYNERGISTIC EFFECTS OF HELIUM AND HYDROGEN IMPLANTATIONS IN TUNGSTEN

G. Yu<sup>1</sup>, L.M. Wang<sup>1</sup>, Q.Z. Yan<sup>2</sup>

<sup>1</sup>Department of Nuclear Engineering and Radiological Sciences, University of Michigan

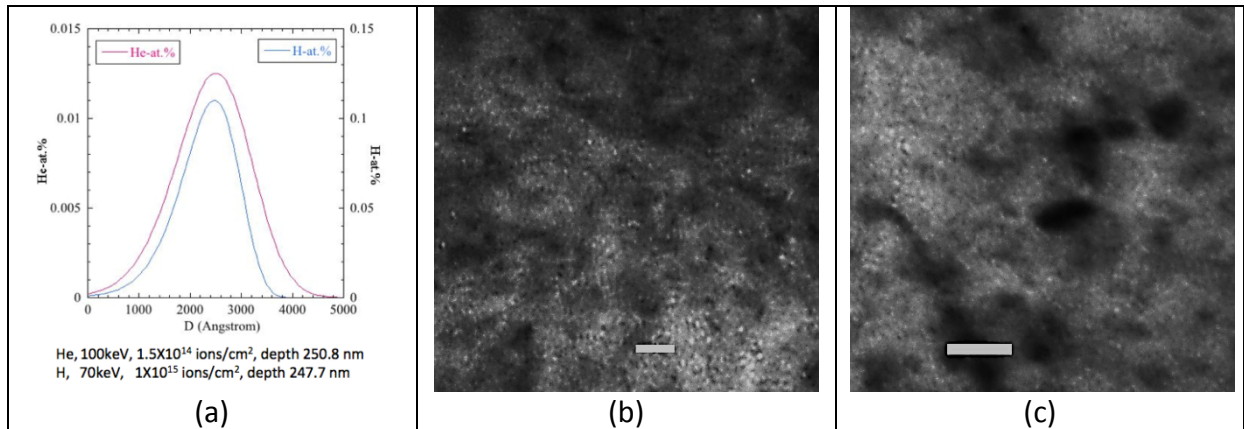
<sup>2</sup>University of Science and Technology, Beijing, China

The University of Science and Technology Beijing (USTB) and the University of Michigan have recently concluded a joint, one-year program on ion irradiation-induced microstructure evolution of tungsten and steels, aimed at studying the behavior of helium and hydrogen in the materials by conducted to microstructure analyses of the helium and hydrogen implanted samples.

Two kinds of tungsten samples, pure and doped tungsten, have been implanted with 100 keV He and 70 keV H, accumulated to 1,000 and 10,000 appm at room temperature, respectively. TEM specimens were prepared by focused ion beam (FIB) milling. The implantation microstructures were examined by TEM.

After implanted 1,000 appm He and 10,000 appm H in pure and drop tungsten at room temperature, it was found that the average cavities size in diameter is less than 1 nm, and the number of density is higher in pure tungsten than in doped tungsten, as shown in figure.

This research was supported by the University of Science and Technology Beijing, China.



Profile results for He and H implantation (a) and microstructures of pure (b), and doped tungsten (c) with 1,000 appm He and 10,000 appm H, respectively. The scale bar is 5 nm.

# EMULATION OF NEUTRON RADIATION-INDUCED SEGREGATION IN FERRITIC-MARTENSITIC ALLOYS WITH ION IRRADIATION

J.P. Wharry, A. Monterrosa, G.S. Was

Department of Nuclear Engineering and Radiological Sciences, University of Michigan

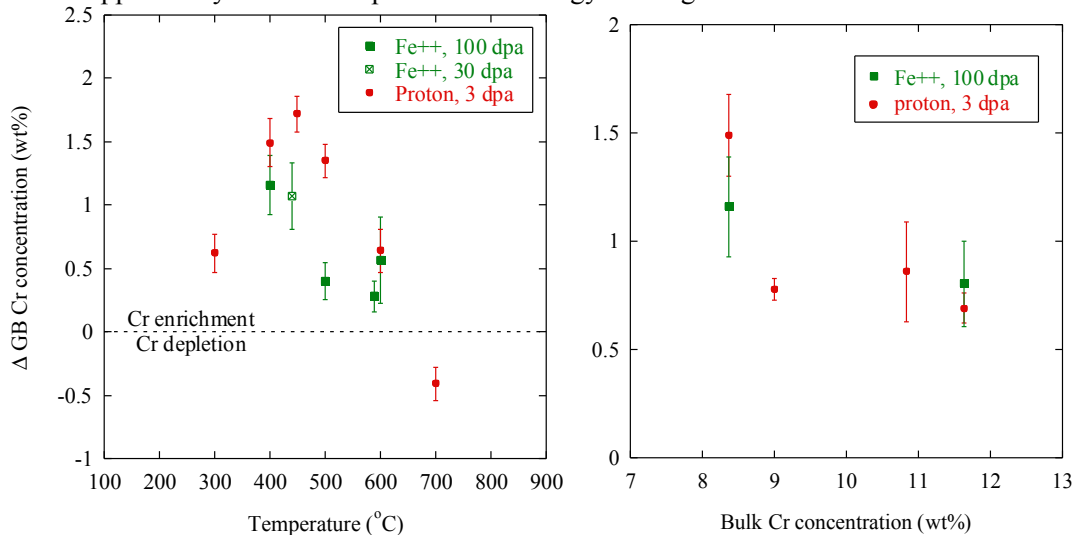
In advanced fast reactors, cladding and structural components made from ferritic-martensitic (F-M) alloys will receive doses of irradiation up to a few hundred dpa, at temperatures  $\sim 400\text{-}500^\circ\text{C}$ . One of the consequences of high-dose irradiation is radiation-induced segregation (RIS) of alloying elements, which could cause embrittlement and materials properties degradation. Because neutron irradiation takes a considerable amount of time ( $\sim 10^7$  dpa/sec dose rate) and causes significant activation, it is desirable to use alternative experimental techniques capable of delivering higher dose rates without residual activity.

This study utilized 5.0 MeV  $\text{Fe}^{++}$  ions, at a dose rate of  $\sim 10^{-3}$  dpa/sec, to irradiate four alloys: T91 (8.37 wt%Cr), HT9 (11.63 wt%Cr), HCM12A (10.83 wt%Cr), and an Fe-9Cr model alloy. Since this work is intended to emulate neutron damage with ions, it is critical to first understand the dose rate dependence of RIS. Unfortunately, RIS measurements from neutron irradiations of these alloys are not yet available. Thus, RIS behaviors from 3 dpa proton irradiations were compared with that from 100 dpa  $\text{Fe}^{++}$  ion irradiations.

The temperature dependence of Cr RIS was evaluated in alloy T91 (left figure); proton irradiation revealed a bell-shaped temperature dependence. A similar trend was observed from 100 dpa  $\text{Fe}^{++}$  ion irradiation, but at a lower magnitude. Proton irradiation of all four alloys (T91, Fe-9Cr, HCM12A, and HT9) at  $400^\circ\text{C}$  (right figure), showed a decrease in the amount of Cr enrichment with increasing bulk Cr concentration. A similar trend was observed with  $\text{Fe}^{++}$  ion irradiation of T91 and HT9 at  $400^\circ\text{C}$ . Thus far, proton and  $\text{Fe}^{++}$  ion irradiations appear to develop RIS to the same extent, and according to the same trends.

Next steps in this project will complete the comparison of RIS dependencies between proton and  $\text{Fe}^{++}$  irradiations. Future work involves the comparison of  $\text{Fe}^{++}$  ion irradiation effects to neutron irradiation effects, including RIS, precipitation, and microstructural evolution.

This work is supported by the U.S. Department of Energy under grant DE-AC07-05ID14517.



Comparison of Cr RIS from 3 dpa proton irradiation to 100 dpa  $\text{Fe}^{++}$  ion irradiation in (left) alloy T91 as a function of temperature, and (right) alloys T91, Fe-9Cr, HCM12A, and HT9 as a function of bulk Cr concentration..

# IN-SITU PROTON IRRADIATION CREEP AND MICROSTRUCTURE OF F-M STEEL T91

C. Xu, G. S. Was

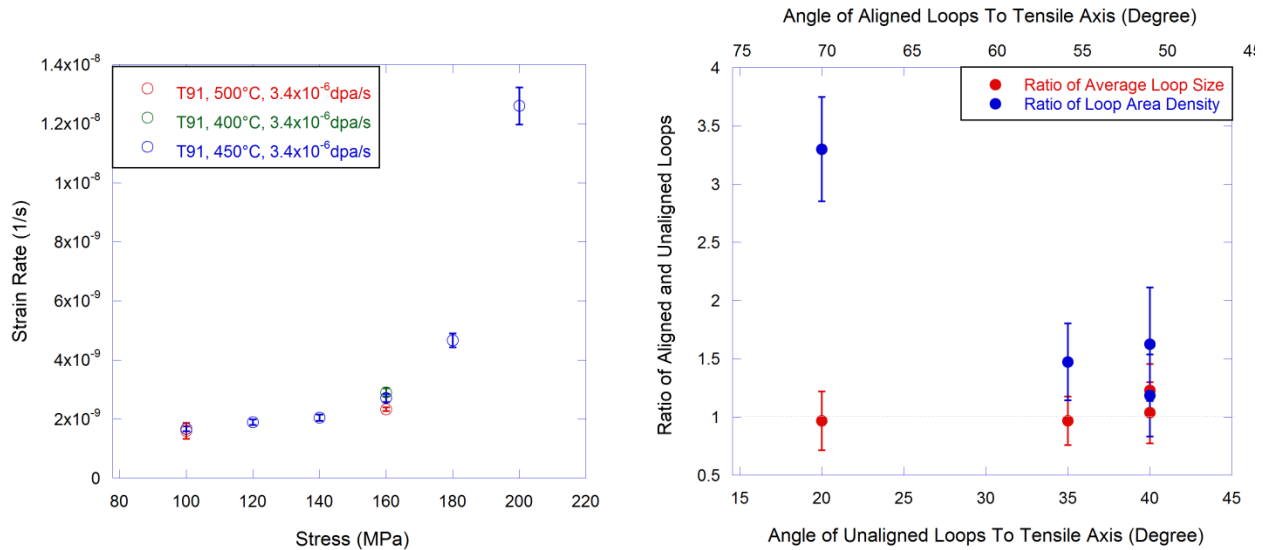
Department of Nuclear Engineering and Radiological Sciences, University of Michigan

In-situ irradiation experiments have been conducted to explore the stress dependence of irradiation creep in F-M alloy T91. Irradiation creep experiments were conducted at 450°C at six different stresses: 100MPa, 120MPa, 140MPa, 160MPa, 180MPa, and 200MPa. Additional creep experiment was conducted at 400°C and 500°C at 160MPa to observe the effect of temperature. Focused Ion Beam (FIB) lift-out samples were made from the irradiated material for microstructure analysis with TEM and STEM.

Irradiation creep rates were obtained by linear fits to in-situ strain measurements by laser speckle extensometer (LSE) for each irradiated condition. The result is plotted in the Figure at left. Preliminary analysis suggested a lack of temperature dependence and deviation from linear stress dependence at stress around 180MPa for irradiation creep.

TEM analysis of the irradiation creep microstructure in the <100> zone axis found large sized  $a_0$ <100> dislocation loops distributed homogenously within the material. Two sets of edge on dislocation loops within a single grain were counted; and their relative ratios were plotted against their orientation to the tensile axis. Four grains in total were analyzed and the ratios of the loop size and loop density are plotted in the Figure at right. No difference in loop size was observed as a function of applied tensile stress, but an increase in loop density was found for loops oriented perpendicular to the tensile axis.

Support for this research was provided by the Department of Energy under NEUP grant DE-AC07-05ID14517.



Stress dependence of irradiation creep (left) and ratio of dislocation loop size and density with respect to the tensile axis for irradiation crept HT9 (right)

# INFLUENCE OF EMBEDDED METALLIC NANOCRYSTALS ON GaAs THERMOELECTRIC PROPERTIES

M.V. Warren<sup>1</sup>, J. C. Canniff<sup>1</sup>, H. Chi<sup>2</sup>, E. Morag<sup>1,3</sup>, C. Uher<sup>2</sup>, R.S. Goldman<sup>1</sup>

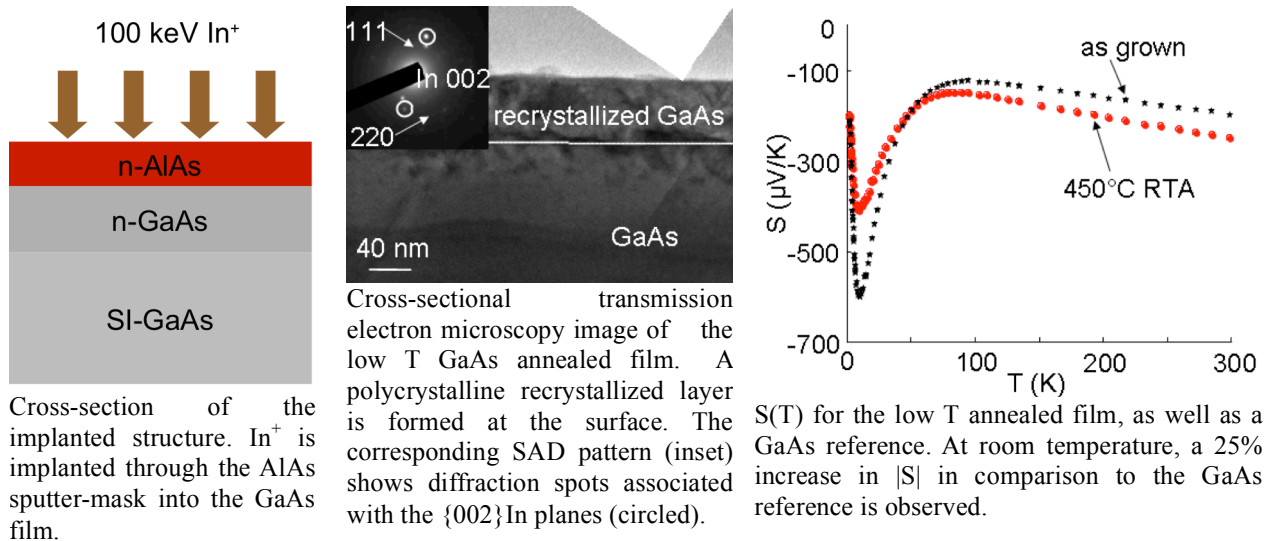
<sup>1</sup>Department of Materials Science and Engineering, University of Michigan

<sup>2</sup>Department of Physics, University of Michigan

<sup>3</sup>Huron High School, Ann Arbor, MI

Nanocomposite materials have been identified as promising candidates for high figure-of-merit thermoelectric materials. Of particular interest is the potential enhancement of the temperature-gradient-induced voltage (the Seebeck coefficient,  $S$ ) using nanoscale inclusions for electron energy filtering. Recently, a new method for the fabrication of embedded metallic and semi-metallic particles has emerged, namely, “matrix-seeded growth,” which consists of ion-beam-amorphization, followed by nanoscale recrystallization via annealing. We fabricate nanocomposites using matrix-seeded growth, which consists of ion irradiation followed by rapid-thermal annealing (RTA). To maximize the retained ion dose, we use a sputter-mask method to preventing sputtering during irradiation.<sup>1</sup> For the case of  $\text{In}^+$  implantation into GaAs at fluences in the range of  $3.8 \times 10^{15}$  to  $3.8 \times 10^{17} \text{ cm}^{-2}$ ,  $|S|$  increases with ion fluence, with an enormous Seebeck coefficient of  $-12 \text{ mV/K}$  at 4 K for the highest ion fluence. For the medium fluence film, a high retained In concentration was observed and the nucleation of metallic In NC within a polycrystalline GaAs matrix was observed for post-irradiation RTA at  $450^\circ\text{C}$ . Interestingly, the presence of In nanocrystals leads to an increase in  $|S|$  of  $50 \mu\text{V/K}$  at 300 K in comparison to an unimplanted film, as well as an increase in free carrier concentration in comparison to GaAs:In films without In nanocrystals.<sup>2</sup> For the case of  $\text{Bi}^+$  implantation into GaAs, an amorphous layer containing crystalline remnants is observed.

This work is supported by the Center for Solar and Thermal Energy Conversion, an Energy Frontier Research Center funded by the U.S. Department of Energy, Office of Science, Office of Basic Energy Science under Award Number DE-SC0000957.



Cross-section of the implanted structure.  $\text{In}^+$  is implanted through the AlAs sputter-mask into the GaAs film.

Cross-sectional transmission electron microscopy image of the low T GaAs annealed film. A polycrystalline recrystallized layer is formed at the surface. The corresponding SAD pattern (inset) shows diffraction spots associated with the  $\{002\}$  In planes (circled).

$S(T)$  for the low T annealed film, as well as a GaAs reference. At room temperature, a 25% increase in  $|S|$  in comparison to the GaAs reference is observed.

# NITROGEN DOPING OF CuInSe<sub>2</sub> FOR THE FORMATION OF HIGHLY CONDUCTIVE THIN FILMS

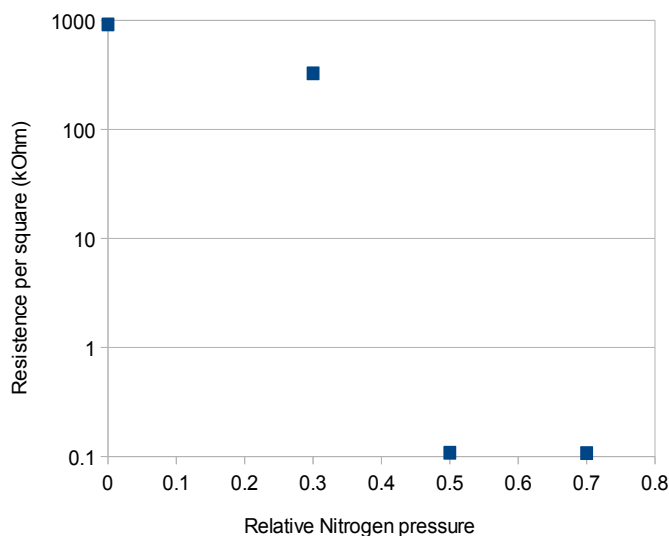
T. Erickson, A. Rockett  
University of Illinois

For this work we dope thin films of CuInSe<sub>2</sub> (CIS) with nitrogen. CIS and related chalcopyrite materials have attracted attention for potential applications in thin film solar cell absorber materials. These materials show good electronic properties in polycrystalline films and have a high tolerance for defects. However, chalcopyrites have been limited by low conductivity, especially for p+ material. In addition, chalcopyrites could potentially be used as contact materials in CdTe thin film solar cells, due to the high work functions of both materials.

The thin films were grown with a hybrid co-sputtering system, using separate copper and indium targets, with a selenium effusion cell. The film stoichiometry was controlled through varying the currents to the Cu and In magnetrons, which, along with an overpressure of Se in the chamber. The substrate temperature was 580°C, measured by pyrometer and a deposition rate of approximately 10 nm/min was achieved. This study added nitrogen to thin films of CIS through activation of N<sub>2</sub> in the sputtering plasma. Part of a Nitrogen free sample was implanted with Nitrogen ions, at 400 keV and with an area density of 5\*10<sup>15</sup> cm<sup>-2</sup>, for use in quantifying the Nitrogen content and conductivity.

SIMS analysis was able to reveal the presence of nitrogen in the thin films, though exact quantities were difficult to determine. Conductivity data revealed an increase in conductivity by a factor of 8.5\*10<sup>3</sup> with increasing nitrogen content in the growth process. The ion implanted sample showed a similar increase in conductivity, increasing by a factor of 4.3\* 10<sup>3</sup>.

We gratefully acknowledge the support of the U.S. Department of Energy Office of Energy Efficiency and Renewable Energy under contract DE-EE0005405.



Decrease in conductivity can be shown with increasing nitrogen content.

# TEACHING

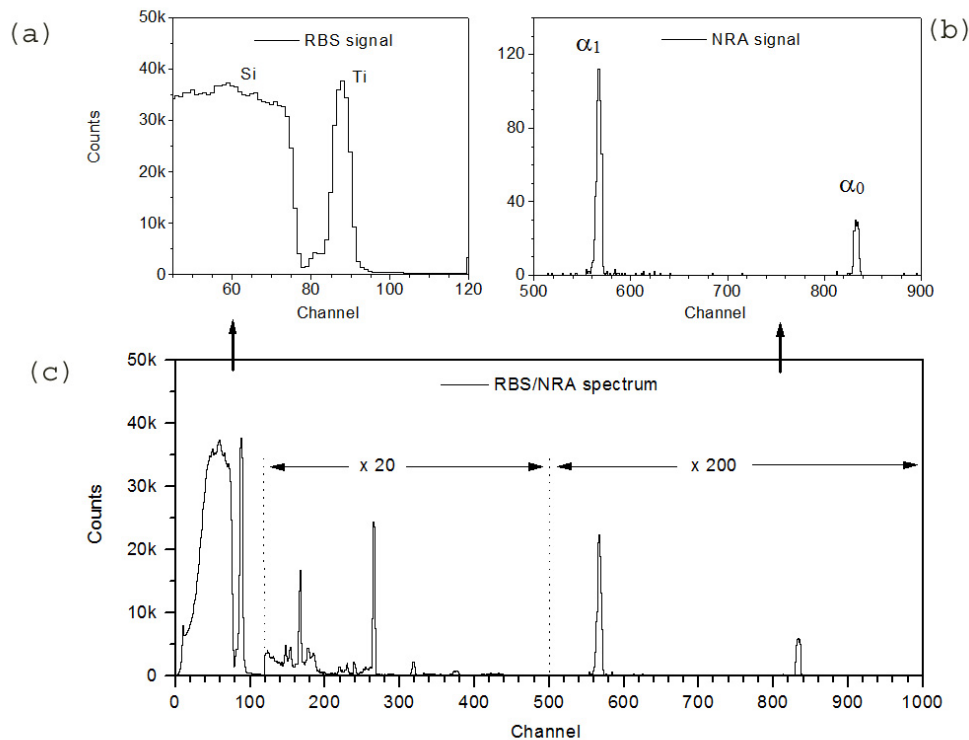
# NERS 425 LABORTORY ON NUCLEAR REACTION ANALYSIS

O. Toader, F. Naab, M. Atzmon

Department of Nuclear Engineering and Radiological Sciences, University of Michigan

For the NERS 425 course, students conducted an experiment to determine the stoichiometry of a  $Ti_xN_y$  sample using the reaction between a deuterium particle and a nitrogen nucleus:  $N^{14}(d,\alpha)C^{12}$ . Nuclear reaction analysis (NRA) is a well-established surface analysis technique. In this method, an energetic particle (deuterium – produced by the Tandem accelerator at MIBL) interacts with the nucleus of an N atom (from the target) to give a reaction product ( $\alpha$  particle) that can be measured. The students also use the backscattered yield from an RBS experiment to determine the amount of Ti in the sample by implementing simulation codes like RUMP or SIMNRA with the given experimental spectrum.

This year the experiment was successfully carried out by all the section of the NERS 425 class. During the first meeting of this class, and prior to the experiment, a short tutorial was given to the students on the accelerator, electronics, detectors, software, and vacuum components. After that, they worked independently in a few groups with just the basic support from the MIBL staff (required in the setup of the ion beam and the collection of the spectra). The students decided on a few parameters of the experiment (beam energy, time for spectrum acquisition, etc.) and after that each group obtains spectra similar to the ones in the figure.



Details of the RBS spectrum (a), the NRA spectrum (b), and typical NRA spectrum for the TiN film obtained during class (c). Conditions: beam energy: 1.4 MeV  $D^+$ , solid angle 5 msr., detector angle  $150^\circ$ .

## PUBLICATIONS AND PRESENTATIONS

G. S. Was and P. L. Andresen, "Irradiation Assisted Corrosion," in Nuclear Corrosion Science and Engineering, D. Feron, Ed., Woodhead Publishing Ltd, Cambridge, UK, 2012.

G. S. Was and R. S. Averback, "Radiation Damage using Ion Beams" Chapter 7 in Comprehensive Nuclear Materials, R. Konings, Ed., Elsevier B. V., 2012.

P. L. Andresen and G. S. Was, "Irradiation-Assisted Stress Corrosion Cracking" Chapter 84 in Comprehensive Nuclear Materials, R. Konings, Ed., Elsevier B. V., 2012.

T. Allen, Y. Chen, D. Guzonas, X. Ren, K. Sridharan, L. Tan, G.S. Was and E. West, "Material Performance in Supercritical Water" Chapter 100 in Comprehensive Nuclear Materials, R. Konings, Ed., Elsevier B. V., 2012.

G. S. Was, T. S. Byun, S. Hu, D. Morgan, Y. Nagai, M. Kerr, *J. Nucl. Mater.*, Volume 425, issues 1-3, *Proceedings of the Symposium on Microstructural Processes in Irradiated Materials*, 2012.

T. Moss, G. S Was, "Dynamic Strain Aging of Nickel-Base Alloys 800H and 690," *Metall. Mater. Trans. A* 43A (2012) 3428-3432.

G. S. Was, D. Farkas, I. M. Robertson, "Micromechanics of Dislocation Channeling in Intergranular Stress Corrosion Crack Nucleation," *Current Opinion in Solid State and Materials Science*, 16 (2012) 134-142.

Z. Jiao, G. S. Was, "Precipitate Evolution in Ion Irradiated HCM12A," *J. Nucl. Mater.*, 425 (2012) 105-111.

J. Wharry, Z. Jiao, G. S. Was, "Application of the Inverse Kirkendall Model of Radiation-Induced Segregation to Ferritic-Martensitic Alloys," *J. Nucl. Mater.*, 425 (2012) 117-124.

E.A. West, M. D. McMurtrey, Z. Jiao, G. S. Was, "Role of Localized Deformation in Irradiation-Assisted Stress Corrosion Crack Initiation," *Metall. & Mater. Trans. A.*, 43A (2012) 136-146.

C. Xu and G. S. Was, "In-situ Irradiation Creep of F-M Alloy T91," TMS Annual Meeting, Orlando FL, March 2012.

A. Campbell and G. S. Was, "Mechanism of Proton Irradiation-induced Creep of Graphite," TMS Annual Meeting, Orlando FL, March 2012.

G. S. Was, Z. Jiao, "Microstructures Resulting from High Dose Irradiation of F-M Alloys and Stainless Steels," Symposium MM: Materials under Extremes, Materials Research Society, 2012.

T. Moss and G. S. Was, "Role of High Nickel and High Cr Austenitic Alloys in IASCC," Meeting on Alloy 800, Toronto, CA, November 2012.

Z. Jiao and G. S. Was, "Progress in Radiation Effects in Reactor Materials through the Consortium for Cladding and Structural Materials," American Nuclear Society, Chicago, IL, June 2012.

G. S. Was, "Challenges to Conducting Materials R&D in Support of Current and Advanced Nuclear Reactor Technologies," Nuclear Reactor Technologies Research, Development and Demonstration Summit, Gaithersburg, MD, March 21, 2012.

G. S. Was and Z. Jiao, "In-situ and Post Irradiation Mechanical Testing of Ion Irradiated Materials," Symposium on Mechanical Performance of Materials for Current and Advanced Reactors, TMS Annual Meeting, Orlando FL, March 2012.

Z. Jiao and G. S. Was, "High Dose Microstructures in Ferritic-Martensitic Alloys," Materials and Fuels for Current and Advanced Nuclear Reactors, TMS Annual Meeting, Orlando FL, March 2012.

E. Beckett, Z. Jiao, K. Sun, G.S. Was, "Role of Helium on Swelling Behavior and Precipitate Formation in Ion Irradiated HT9 Steel," Poster presentation at Engineering Graduate Symposium, University of Michigan, October, 2012, Ann Arbor, MI

Stephen S. Raiman, Alexander Flick, Ovidiu Toader, Fabian U. Naab, Nassim A. Samad, Zhijie Jiao, Gary S. Was, "A Method for In-Situ Studies of Irradiation Accelerated Corrosion," ANS Conference, May 2012, Chicago, IL

S. Dwaraknath, & G. S. Was, (2011). Silver Diffusion in PyC Coated  $\beta$ -SiC. Presented at the TMS 2012, Orlando, FL.

A.A. Campbell, G.S. Was, "Mechanism of Proton Irradiation-Induced Creep of Pyrolytic Carbon", TMS Annual Meeting, Orlando, FL, March 11-15, 2012.

Cheng Xu, Gary S. Was, "In-situ Irradiation Creep of F-M Alloy T91", TMS Conference, Orlando, FL, March 11 2012.

Cheng Xu, Gary S. Was, "Irradiation Creep and Microstructure of F-M Alloy T91", ANS Conference, Chicago, IL, June 25 2012.

Z. Jiao, G.S. Was, T. Allen, D. Morgan, A. Motta, B. Wirth, etc "Microstructure and Property Evolution in Advanced Cladding and Duct: Materials under Long-Term and Elevated Temperature" ANS 2012, Chicago, IL. June 26, 2012

Z. Jiao, G.S. Was, "High Dose Microstructures in Ferritic-Martensitic Alloys", School of Energy Research, Xiamen University, May 3, 2012

Z. Jiao, G.S. Was "Strategies for Studying Irradiation Effects in Materials using Ions", National Center for Materials Safety, U. of Sci. & Tech. Beijing, April 25, 2012

Z. Jiao and G.S. Was, "High Dose Microstructures in Ferritic-Martensitic Alloys" Materials and Fuels for the Current and Advanced Nuclear Reactors, TMS2012, Orlando, FL. March 11-15, 2012.

O.F. Toader and F.U. Naab, "Designing a Multiple Ion Beam Facility," Symposium of North Eastern Accelerator Personnel (SNEAP), Padova, IT, Sept 30 – Oct. 5, 2012.

C. Chen, J. Hwang, A. S. Teran, J. Foley, and J. D. Phillips, "Growth and optoelectronic properties of ZnTe with dilute oxygen," the 54<sup>th</sup> Annual Electronic Materials Conference, Pennsylvania State University, State College, Pennsylvania, June 2012.

J. Phillips, C. Chen, W. Wang, V. Stoica, R. Clarke, E. Antolin, E. Lopez, I. Ramiro, E. Hernandez, I. Artacho, A. Marti and A. Luque, "Intermediate band solar energy conversion in ZnTe:O," European Materials Research Society Spring Meeting, Strasbourg, France (2012).

C. Chen, S. Kim, X. Pan and J. Phillips, "Dilute oxygen incorporation in ZnTe by plasma-assisted molecular beam epitaxy," North American Conference on Molecular Beam Epitaxy, Stone Mountain Park, Georgia (2012).

E. Antolin, I. Ramiro, E. Lopez, E. Hernandez, I. Artacho, C. Tablero, A. Marti, A. Luque, C. Chen, J. Foley and J. D. Phillips, "Intermediate band to conduction band optical absorption in ZnTeO", 38th IEEE Photovoltaic Specialists Conference, Austin, Texas (2012).

D.F. Reyes, F. Bastiman, L. D. Blanco, D. L. Sales, and D. Gonzales, presented at the 15th European Microscopy Congress, Manchester, United Kingdom (2012).

M.V. Warren, A.W. Wood, J.C. Canniff, F. Naab, C. Uher, and R.S. Goldman, Appl. Phys. Lett. **100**, 102101 (2012).

M.V. Warren, J.C. Canniff, H. Chi, E. Morag, F. Naab, C. Uher, and R.S. Goldman, "Influence of Embedded Indium Nanocrystals on GaAs Thermoelectric Properties," submitted.